Research Paper

GEOSPHERE

GEOSPHERE, v. 13, no. 6

doi:10.1130/GES01493.1

9 figures; 1 supplemental file

CORRESPONDENCE: cbzaffarana@gmail.com

CITATION: Zaffarana, C.B., Somoza, R., Orts, D.L., Mercader, R., Boltshauser, B., González, V.R., and Puigdomenech, C., 2017, Internal structure of the Late Triassic Central Patagonian batholith at Gastre, southern Argentina: Implications for pluton emplacement and the Gastre fault system: Geosphere, v. 13, no. 6 doi:10.1130/GES01493.1.

Received 30 December 2016
Revision received 25 July 2017
Accepted 12 September 2017

Internal structure of the Late Triassic Central Patagonian batholith at Gastre, southern Argentina: Implications for pluton emplacement and the Gastre fault system

Claudia B. Zaffarana[1], Rubén Somoza[2,†], Darío L. Orts[1], Roberto Mercader[3], Bárbara Boltshauser[2], Víctor Ruiz González[2], and Carla Puigdomenech[2]

[1]Instituto de Investigación en Paleobiología y Geología (IIPG), Consejo de Investigaciones Científicas y Técnicas (CONICET). Av. Julio A. Roca 1242 General Roca (8332), Provincia de Río Negro 8332, Argentina
[2]Instituto de Geociencias Básicas, Aplicadas y Ambientales de Buenos Aires (I.G.E.B.A.), Consejo Nacional de Investigaciones Científicas y Técnicas (CONICET), Intendente Güiraldes 2160, Pabellón II, Piso 1, Ciudad Universitaria, Buenos Aires 1428, Argentina
[3]Departamento de Física, Facultad de Ciencias Exactas, Universidad Nacional de La Plata, Buenos Aires 1900, Argentina

ABSTRACT

The Central Patagonian batholith (CPB) comprises two Late Triassic calcalkaline plutonic suites (the Gastre superunit of 221 ± 2 Ma and the Lipetrén superunit of 215 ± 1 Ma) which have been interpreted as a record of major dextral motion along the transcontinental NW-SE–striking subvertical Gastre fault system in Jurassic times. We performed a detailed study of the internal structure of the CPB through structural and anisotropy of magnetic susceptibility (AMS) techniques. The Gastre superunit reveals a very consistent pattern of NW-SE–striking steeply dipping magmatic foliations. Tectonic fabrics within the CPB are scarce and generally parallel to the magmatic fabrics. The magmatic and solid-state lineations within the CPB are steeply, intermediately, or shallowly plunging. The combination of flattened magmatic and solid-state fabrics with subvertical orientations and with steep to shallow lineations, together with the kinematic indicators in two mylonite belts with suspected CPB protoliths, suggests that the Gastre superunit was emplaced within a sinistral transpressive regime. The shallower stocks of the Lipetrén superunit are more isotropic and have magmatic fabrics associated with magma chamber dynamics. The deformation of the CPB is coaxial with the late Paleozoic deformation in the hosting Calcatapul Formation. The late Paleozoic deformation in the North Patagonian Massif generated widespread NW-SE subvertical fractures which could have aided the emplacement of the CPB. The internal structure of the CPB does not support a model of dextral strike-slip movements on major Jurassic faults.

INTRODUCTION

The Central Patagonian batholith (CPB; Fig. 1A; Rapela et al., 1991, 1992; Zaffarana et al., 2014) is a suite of Late Triassic calcalkaline plutons that represents a key element in paleogeographic models of pre-Gondwana breakup, as it was emplaced during the transition between the Gondwanide (late Paleozoic) and the Andean (Jurassic to present) tectonic cycles in South America. The emplacement of the CPB has been inferred as syntectonic with the activity of the Gastre fault system, a controversial NW-SE subvertical structure that has been conceived as a major dextral fault cross-cutting Patagonia (Fig. 1A; Rapela et al., 1991, 1992; Rapela and Pankhurst, 1992; Marshall, 1994; König and Jokat, 2006; Martin, 2007; Riley et al., 2016). The Gastre fault system was widely invoked to restore Patagonia to achieve a tectono-stratigraphic correlation between the Paleozoic successions from the Malvinas-Falkland islands and the Cape fold belt of South Africa (Marshall, 1994; Storey et al., 1999; Macdonald et al., 2003; Hole et al., 2016). This correlation also requires ~100° clockwise rotation of the Malvinas-Falkland islands, which in turn has been independently supported by paleomagnetic results from NE-SW–trending Jurassic dikes cropping out in the islands (Taylor and Shaw, 1989). According to this model, almost all the dextral motion through the Gastre fault system must be younger than 190–180 Ma, which is the age of the paleomagnetically studied dikes (Mussett and Taylor, 1994; Stone et al., 2008, 2009; Hole et al., 2016). Figure 1A shows the inferred trace of the Gastre fault system passing along the outcrops of the Late Triassic CPB. Recent paleomagnetic data from the overlying Lonco Trapial Formation (Fig. 1B) indicate that no clockwise tectonic rotations took place in the Jurassic through the Gastre district (Zaffarana and Somoza, 2012).

Furthermore, local mesoscale geological observations in the type locality of the Gastre fault system argue against the idea that the CPB has been affected by continental-scale Jurassic dextral shearing (von Gosen and Loske, 2004; Zaffarana et al., 2010, 2014). However, a comprehensive structural characterization of the CPB has remained a pending task. In this contribution, we present the results of a study of the internal structure of the plutons that compose this batholith. In many sectors of the batholith, the determination of foliation and lineation is difficult because of the preponderance of

[†]Deceased

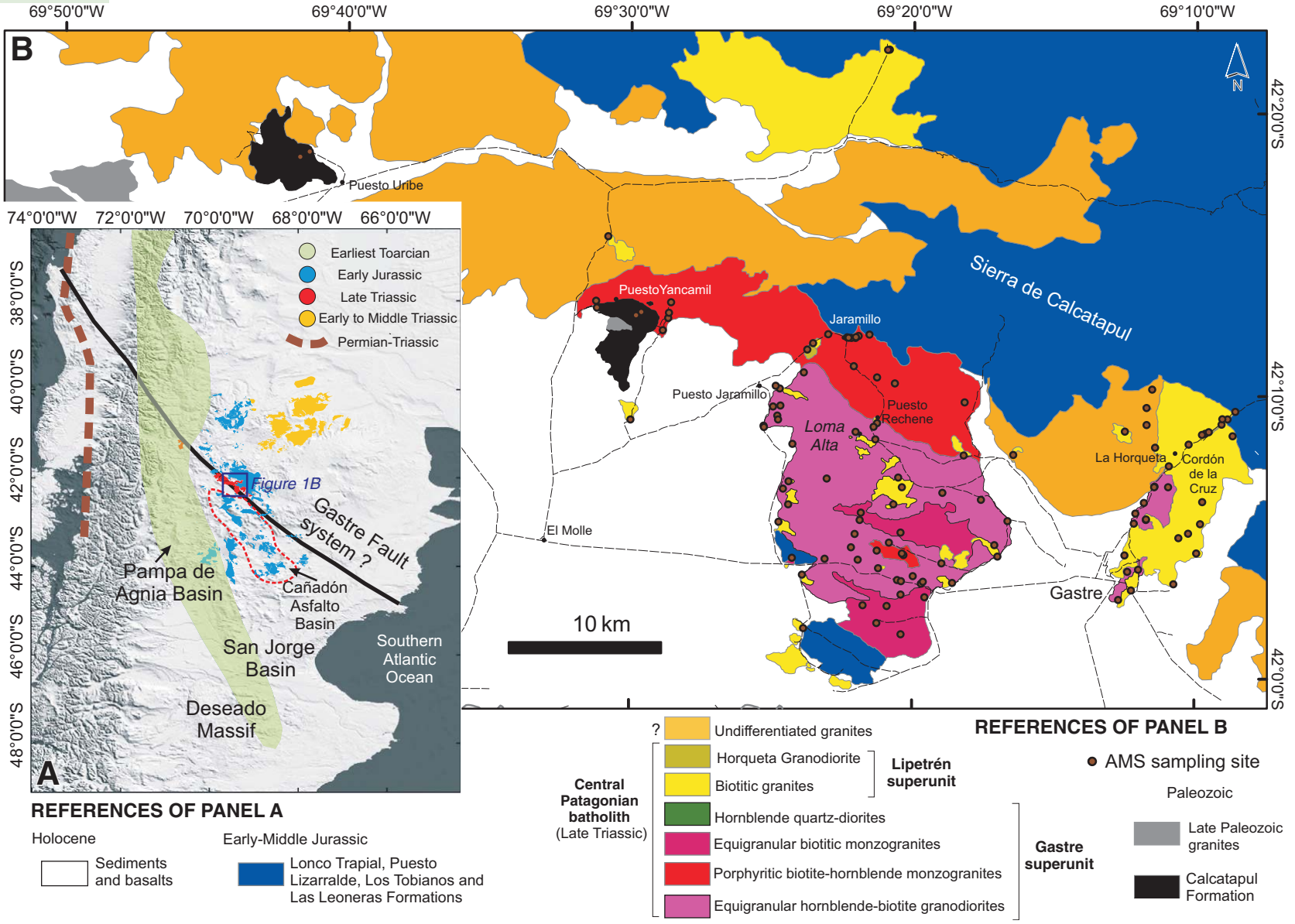

Figure 1. (A) Regional map of southern South America showing the inferred trace of Gastre Fault System. The figure shows that it does not deflect the late Pliensbachian-Toarcian deposits of the Pampa de Agnia Basin (Lesta et al., 1980; Uliana and Biddle, 1978; Uliana and Legarreta, 1999; Vicente, 2005), and that it traverses the San Jorge basin without any offset. The outcrops of the Late Triassic Central Patagonian batholith are located along its trace. (B) Regional map of the Central Patagonian batholith with the main distribution of sampling sites and with inset of the area studied in detail. GFS—Gastre fault system; AMS—anisotropy of magnetic susceptibility. Based on von Gosen and Loske (2004), Zaffarana et al. (2014), and Cábana et al. (2017).

magmatic fabrics and because of the common presence of equigranular and in some cases fine-grained plutonic rocks. To solve this, we performed anisotropy of magnetic susceptibility (AMS) measurements in systematically distributed sites (as much as possible) over an area of ~400 km^2 around the Gastre locality. The integration of the AMS results with our more local meso- and microscale structural observations results in a suitable picture of the internal structure of the plutonic rocks (Fig. 1B), which has implications to magmatic processes.

GEOLOGICAL SETTING

The CPB is composed of Late Triassic (time scale of Cohen et al., 2016) calcalkaline plutons (Rapela et al., 1991, 1992; Rapela and Pankhurst, 1992). These granitoids have initial Sm/Nd and $^{87}Sr/^{86}Sr$ isotopic ratios intermediate between the primitive, mantle-derived isotopic signatures of the Andean arc-related batholiths and that of the more evolved, widely distributed Permian granitoids of northern Patagonia (Rapela et al., 2005; Pankhurst et al., 2006). These intermediate ratios reflecting mantle and crustal contributions led previous authors to consider the plutons of the CPB as "modified I-type" (Pankhurst, 1990; Rapela et al., 1991, 1992; Rapela and Pankhurst, 1992).

Exposure of the CPB is excellent, with an overall vertical relief of ~800 m. Access is difficult toward the north, where the granites are covered by the Lower Jurassic volcanic rocks of the Lonco Trapial Formation (Fig. 1B). The CPB is primarily comprised of diorites to granites of the older Gastre superunit, which are in turn intruded by the granites of the Lipetrén superunit (Rapela et al., 1991, 1992; Zaffarana et al., 2014).

The oldest unit of the Gastre superunit comprises equigranular hornblende-biotite granodiorites (Zaffarana et al., 2014). These granodiorites pass gradually to porphyritic biotite-hornblende monzogranites (Zaffarana et al., 2014). Another unit in the Gastre superunit is composed of equigranular biotitic monzogranites, which form stocks of light pink, medium- to coarse-grained equigranular monzogranites that intrude both the equigranular hornblende-biotite granodiorites and the porphyritic biotite-hornblende monzogranites (Zaffarana et al., 2014). The Gastre superunit is intruded by at least three stocks of dioritic to quartz-monzodioritic composition and by dioritic to quartz-dioritic dikes. The stocks and the dikes comprise the hornblende quartz diorites (Zaffarana et al., 2014). The Lipetrén superunit is predominantly composed of more evolved granitic rocks, mostly of biotitic monzo- and syenogranites that intrude all of the units of the Gastre superunit (Zaffarana et al., 2014). Big tabular bodies of the biotitic granites are particularly well exposed to the east of Gastre village at the Cordón de la Cruz (Fig. 1; Zaffarana et al., 2014). Volcanic to subvolcanic equivalents of these granites are difficult to find. Possible volcanic equivalents are the felsites that crop out in several places of the northern studied sector, in all cases close to the contact with the overlying Lonco Trapial Formation (Lower Jurassic) and which were mentioned by Rapela et al. (1991). They are pink to brown aplitic rocks mostly composed of small crystals of quartz and feldspar. These rocks could signal the highest structural level exposed in the batholithic system. The only clearly extrusive rock that could be associated with the magmatic system of the CPB corresponds to a meter-scale outcrop (42°01.169′S, 69°23.198′W) of a gray ignimbrite with eutaxitic texture and a rhyolitic to dacitic composition.

The Gastre superunit yields a Rb-Sr isochron age of 222 ± 3 Ma (data from Rapela et al. [1992] reinterpreted by Zaffarana et al. [2014]) and a U-Pb zircon age of 221 ± 2 Ma that was mentioned (without providing analytical data) by Rapela et al. (2005). The Gastre superunit also yields an $^{40}Ar/^{39}Ar$ stepwise biotite cooling age of 213 ± 5 Ma (Zaffarana et al., 2014). With respect to the Lipetrén superunit, a recently reported U-Pb SHRIMP (sensitive high-resolution ion microprobe) age of 215 ± 1 Ma for its monzogranites (Lagorio et al., 2015) suggests that the previous $^{40}Ar/^{39}Ar$ stepwise biotite cooling age of 206 ± 4 Ma and the Rb/Sr isochron age of 206.4 ± 5.3 Ma discussed by Zaffarana et al. (2014) represent cooling ages associated with moderate cooling rates.

The Lipetrén superunit also comprises the Horqueta Granodiorite (Rapela et al., 1991, 1992), a set of biotitic granodiorites whose age had remained poorly constrained (Zaffarana et al., 2014) until the acquisition of a new U-Pb zircon SHRIMP crystallization age of 213 ± 2 Ma (Lagorio et al., 2015). This age overlaps with the $^{40}Ar/^{39}Ar$ stepwise biotite cooling age of 211 ± 2 Ma reported by Zaffarana et al. (2014). The crystallization ages of the Gastre and Lipetrén superunits suggest that a time span of ~7 m.y. elapsed between their emplacements.

Outcrops of host rock of the CPB are scarce because, with the exception of the metamorphic Calcatapul Formation (Proserpio, 1978), possible host rocks would be hard to identify in the field because they belong to granites of the previous late Paleozoic intrusive cycle (the Permian granitoids of the Mamil Choique Formation; Cerredo and López de Luchi, 1998; López de Luchi and Cerredo, 2008). The Paleozoic Calcatapul Formation crops out exclusively in the southern side of the Sierra de Calcatapul (near Puesto Yancamil and Puesto Uribe; Fig. 1). It consists of a steeply dipping, dynamically metamorphosed succession of metavolcanic rocks with thin intercalations of phyllites and metaconglomerate lenses (Proserpio, 1978; von Gosen and Loske, 2004; Zaffarana et al., 2010). The Calcatapul Formation shows a subvertical, NW-SE penetrative S_1 foliation developed under greenschist facies conditions that is almost parallel to the bedding planes (von Gosen and Loske, 2004; Zaffarana et al., 2010). The lineation is subvertical at Puesto Yancamil and subhorizontal a few kilometers northwards (von Gosen and Loske, 2004; Zaffarana et al., 2010; P53 and P156 in Table S1 in the Supplemental Materials[1]), suggesting that the S_1 planes either formed under partitioned transpression or were produced by separate deformation events. The Permian biotitic porphyritic Yancamil Granite (von Gosen and Loske, 2004) intrudes the Calcatapul Formation at Puesto Yancamil. The Yancamil Granite and its host bear a tectonic foliation and lineation with the same orientation (von Gosen and Loske, 2004; Zaffarana et al., 2010; the granite corresponds to site P148 in Table S1 [see footnote 1]). At Puesto Yancamil, the NW-SE steep foliation and the steeply dipping lineation of Calcatapul Formation were interpreted as the result of downfaulting

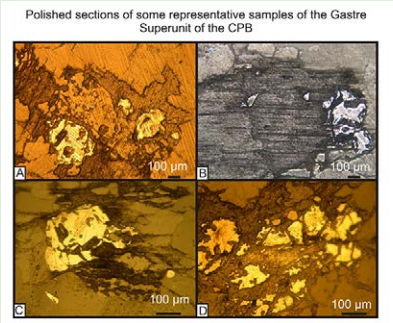

[1]Supplemental Materials. Rock-magnetic studies of representative samples, AMS results, and a graph reinterpreting the emplacement pressure of the CPB. Please visit http://doi.org/10.1130/GES01493.S1 or the full-text article on www.gsapubs.org to view the Supplemental Materials.

deformation or of oblique (sinistral) displacements (Franzese and Martino, 1998; von Gosen and Loske, 2004; Zaffarana et al., 2010). Additionally, some insights about the host rock near the town of Gastre are given by small (decameter- to hectometer-scale) stoped blocks (Yoshinobu et al., 2009) of metamorphic rocks enclosed within the CPB (Zaffarana et al., 2012, 2014).

STRUCTURAL GEOLOGY

Microstructural observations were performed on a collection of 110 thin sections. Samples from outcrops having visible foliation were oriented according to planar and, whenever possible, linear structures observed in the field. Fabrics of the CPB range from pre–full crystallization state to superimposed low-temperature solid-state deformation. For practical purposes, the outcrops selected for AMS studies were classified as exhibiting magmatic or solid-state fabrics ("M" or "S", respectively, in Tables S1–S3 [see footnote 1]) on the basis of observable megascopic structures in the field.

Sites involved in the magmatic, or M, field classification (example in Figs. 2A–2D) comprise rocks whose microstructures are purely magmatic, submagmatic (with low melt percent; Paterson et al., 1989; Bouchez et al., 1992; Cruden et al., 1999), and/or with a mild overprinting of solid-state deformation, the latter formed especially in high-temperature conditions near the solidus temperature (Blumenfeld et al., 1986; Gapais and Barbarin, 1986; Mainprice et al., 1986; Paterson et al., 1989; Figs. 2A–2D). The high-temperature solid-state fabrics are in all cases coaxial with the magmatic fabrics.

In contrast, the rocks from sites classified as exhibiting S fabrics show solid-state deformation visible at hand-sample scale (Figs. 2E–2H). In this case, microstructures involve grain-size reduction and the development of moderate to strong mineral foliation and, in some cases, mineral lineation (Fig. 2F). Microstructures include subgrains in quartz and incipient bulging of and microfracturing in feldspar. These processes which result in S fabrics occur at relatively low- to medium-temperature conditions (300–500 °C) and/or at fast strain rates (Hirth and Tullis, 1992; Tullis et al., 2000). However, when deformation starts at high-temperature conditions and almost continuously follows up to low-temperature conditions (as is a common case in deformed granites), the resulting fabrics are classified in the field as S as well (Figs. 2G–2H). Mylonitic fabrics are a special type of S fabrics.

Magmatic Fabrics

In the CPB as a whole, magmatic fabrics (M fabrics) predominate over the solid-state fabrics (S fabrics; Fig. 2I). The orientation of the magmatic and tectonic foliations and lineations measured in the field are detailed in Tables S1–S3 (see footnote 1). The magmatic foliations are usually well defined and mostly subvertical, whereas the magmatic lineations are rarely observable. The dioritic dikes belonging to the hornblende quartz diorites are generally subvertical, with variable strike, and dispersed throughout the Gastre superunit. We have sampled 11 dikes, all of them subvertical, with predominantly NE-SW or NNE-SSW strike (six dikes), but NW-SE (three dikes) and N-S strikes (two dikes) also occur (Table S2 [see footnote 1]). Six dikes have magmatic fabric and five have low-temperature solid-state deformation; the solid-state deformational fabrics all have steep foliation planes (70° or higher; Tables S2–S3 [see footnote 1]).

Solid-State Fabrics

Ductile shear zones were observed in several localities (Fig. 2I). The high- and low-temperature deformation present at Puesto Yancamil and at Puesto Jaramillo was described by von Gosen and Loske (2004) and by Zaffarana et al. (2010), and the observations in Puesto Yancamil were summarized previously. In this work, we contribute the description of the deformation and kinematics of seven additional mylonitic zones. The first one corresponds to the Calcatapul Formation at Puesto Uribe (Fig. 1; P139 in Table S1 [see footnote 1]). There, metaconglomerate layers have a NW-SE subvertical foliation and a lineation plunging 50° toward the NW with an oblique (sinistral) sense of shear. The other shear zones are developed in granites of the CPB, where three of them are assigned to the Gastre superunit and the other two to the Lipetrén superunit (Table S3 [see footnote 1]; Fig. 3). The thickest (~100 m 215 thick) mylonitic zone has oblique (sinistral) kinematics and is located near Puesto Uribe ("Uribe 216 mylonite" at P138 in Table S3 [see footnote 1]). It has a suspected Gastre superunit protolith. There, the tectonic foliation strikes NNW-SSE and the lineation plunges steeply (60°–70°) toward the NNW (Fig. 3A). K-feldspar and granitic porphyroclasts of different sizes (from millimeters up to 50 cm) are surrounded by strain shadows defining δ-type or, more commonly, σ-type microstructures, which suggest uplift of the southwest block with respect to the northeast block with a sinistral shear component (Figs. 3A–3D). About 500 m to the northwest of this shear zone, the hosting metapyroclastic rocks of Calcatapul Formation also appear mylonitized (site P139, Table S1 [see footnote 1]), with the foliation and lineation parallel to that observed in the above-mentioned ~100-m-thick mylonite. The metapyroclastic rocks contain angular porphyroclasts of quartz, microcline, and zonal plagioclase immersed in a matrix composed of quartz, sericite, and chlorites with evidence of dynamic recrystallization. Porphyroclasts in the metapyroclastic rocks have straight grain boundaries, and nearly all are surrounded by strain shadows and by quarter mats (Hanmer and Passchier, 1991).

The other shear zones that traverse the granites of the CPB are much thinner and of lesser importance. The mylonites near Puesto Rechene have a NW-SE–trending subvertical mylonitic foliation and form a ~15–20-m-wide zone with a shallowly plunging lineation defined by elongated quartz and feldspar grains (Figs. 3E–3H; "Rechene mylonite" at P143 in Table S3 [see footnote 1]). Sinistral sense of shear is suggested by the development of S-C′ planes. The ductile shear zone near La Horqueta has a mylonitic foliation in

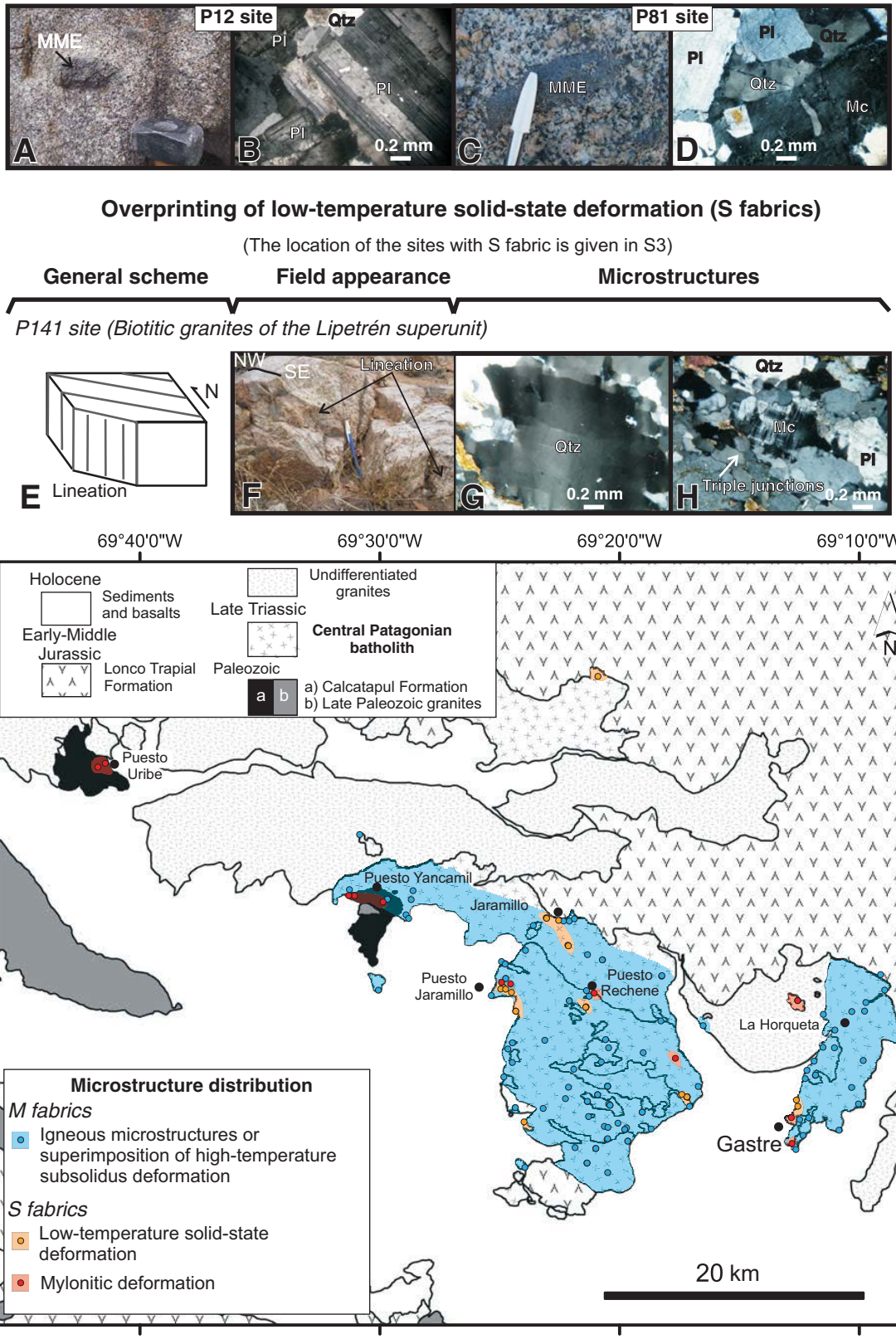

Figure 2. General classification of microstructures of the Central Patagonian batholith, where the location of the magmatic (M) fabrics can be found in Table S2 (see footnote 1) and the location of the solid-state (S) fabrics can be found in Table S3 (see footnote 1). (A)–(B) Field appearance (A) and magmatic microstructures (B) at site P12, where grain boundaries are mostly straight and quartz shows only very weak undulose extinction. (C) Field appearance at site P81. (D) High-temperature solid-state deformation at site P81 evidenced by chessboard extinction in quartz and by K-feldspar inversion to microcline. (E)–(G) General description, field appearance, and microstructures of the biotitic granites of the Lipetrén Superunit bearing low-temperature solid-state deformation at P141 site. (E) General scheme of low-temperature solid-state deformation in the Lipetrén superunit at site P141. (F) Field appearance of the steeply dipping NW-SE foliation planes and the subvertical lineation defined by elongated biotites, quartz, and feldspars. (G) Quartz porphyroclast with elongated subgrains and triple junctions between grains. (H) Quartz, plagioclase, and microcline recrystallized grains. All photomicrographs were taken under crossed polars, and mineral abbreviations are after Kretz (1983). Qtz—quartz, Pl—plagioclase, Mc—microcline; MME—mafic microgranular enclaves. (I) Hand-contoured map of microstructure distribution.

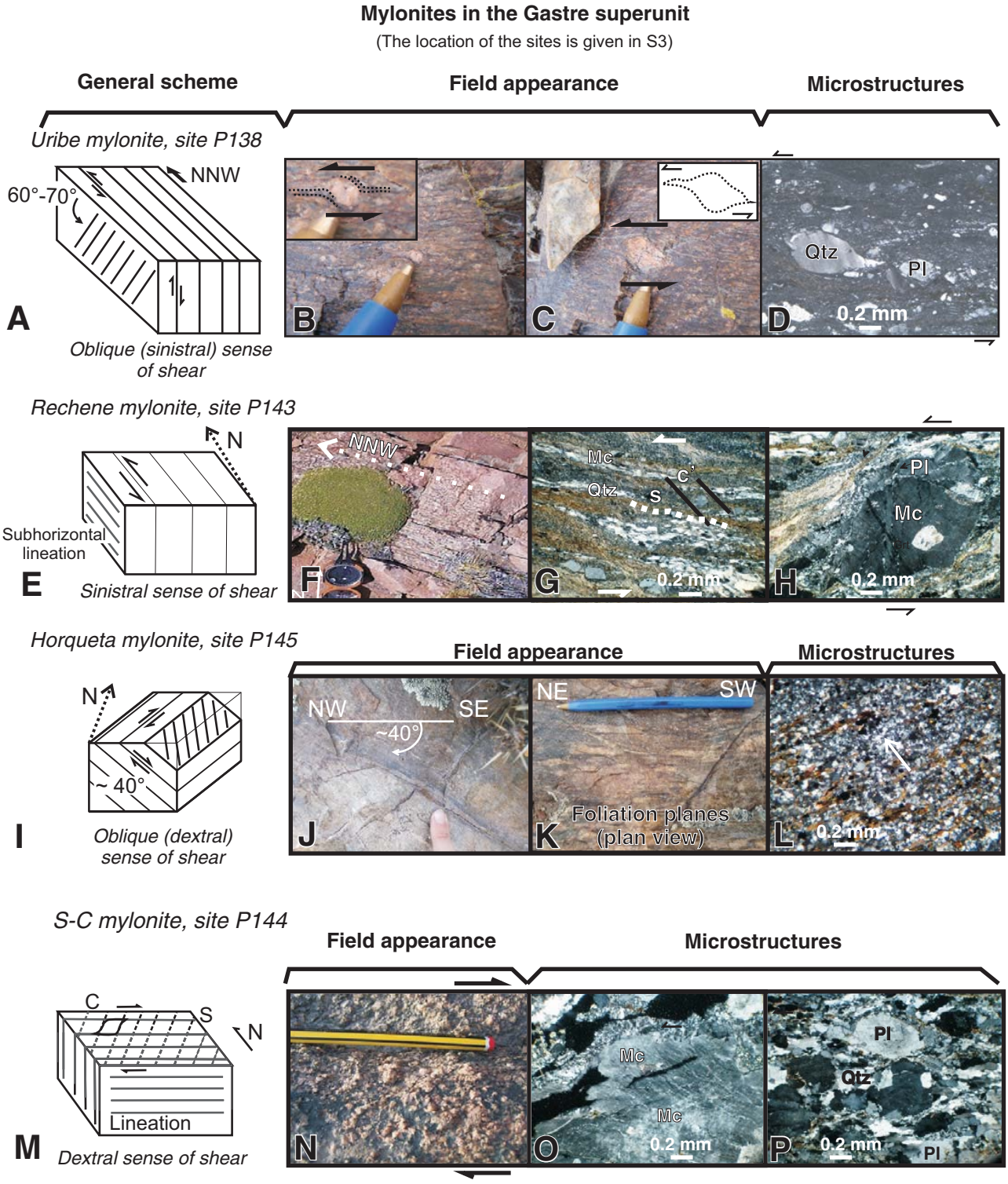

Figure 3. Mylonites in the Gastre superunit; their location can be found in Table S3 (see footnote 1). (A)–(D) General scheme, field appearance, and microstructures of the mylonites of Puesto Uribe at site P138. (A) Outcrop scheme of the Uribe mylonites showing NNW-SSE subvertical foliation with a steeply dipping lineation plunging 60°–70° to the NNW. (B)–(C) σ-type porphyroclasts of K-feldspar recording sinistral sense of shear immersed in a dark-colored aphanitic matrix. (D) Sinistral sense of shear recorded by σ-type quartz porphyroclasts with deformation bands. See also the plagioclase porphyroclast with polysynthetic twinning and the recrystallized matrix composed of quartz, feldspars, and micas. (E)–(H) General scheme, field appearance and microstructures of the mylonites at Puesto Rechene at site P143. (E) General scheme of Rechene mylonites. (F) Field appearance of the regular subvertical NNW-SE foliation planes. (G) S-C′ structure defining sinistral sense of shear. (H) Microcline porphyroclast with recrystallized borders surrounded by small quartz, microcline, and plagioclase subgrains with a sinistral sense of shear. (I)–(L) General scheme, field appearance, and microstructures of the mylonites near La Horqueta. (I) General scheme of the Horqueta mylonites, with NE-SW foliation dipping to the SE and a SE-plunging lineation with an oblique (dextral) sense of shear. (J)–(K) Foliation planes perpendicular (J) and parallel (K) to the strike. (L) Equidimensional aggregates of quartz and feldspar suggest post-kinematic annealing. White arrow in (L) signals triple junctions within minerals (static recrystallization). (M–P): General scheme, field appearance, and microstructures of the mylonites with S-C structure at site P144. (M) General scheme of the S-C mylonites at site P144 with subvertical E-W foliation, subhorizontal lineation, and a dextral sense of shear. (N) General appearance in the field. (O) Microcline porphyroclasts with flame perthites surrounded by recrystallized bands of subgrains. (P) Plagioclase and quartz porphyroclasts and bands of subgrains. Mineral abbreviations are after Kretz (1983) Qtz—quartz; Pl—plagioclase; Mc—microcline.

a ~10-m-wide zone, with NE-SW strike and a moderate dip (40°–50°) to the SE (Figs. 3I–3L; "Horqueta mylonite" at P145 in Table S3 [see footnote 1]). An oblique (dextral) sense of shear was detected parallel to the moderately SW-plunging mineral lineation. Foliation is regular and defined by lenses of quartz and feldspars with dynamic recrystallization surrounded by bands of biotite and opaque minerals. The rocks are strongly annealed, as quartz and feldspars originally formed by dynamic recrystallization appear now as a mosaic of equigranular grains free of deformation with straight grain boundaries meeting at triple junctions.

The equigranular hornblende-biotite granodiorites of the Gastre superunit are mylonitized at P144 (Figs. 3M–3P; "S-C mylonite" in Table S3 [see footnote 1]) with an E-W subvertical foliation and a subhorizontal mineral lineation defined by elongated quartz and biotite crystals. The shear zones are thin and parallel, between 50 and 20 cm wide. The S-C structure defines a dextral sense of shear.

The Lipetrén superunit is mylonitized in two mylonitic zones located near the east of the Gastre village. The northern one (site P59 in Table S3 [see footnote 1]; Figs. 4A–4D) trends NNW-SSE and dips moderately to the west (~50°–70°), its width is 10 m, and the mylonitic foliation is defined by the alternation of lighter bands composed of quartz and micas with darker bands composed of opaque minerals and micas. The lineation plunges ~30° to the NW. S-C′ microstructures suggest oblique (sinistral) uplift of the western block with respect to the eastern one. The mylonitic foliation is cut by low-angle brittle fractures filled with quartz, feldspar, and epidote which developed in a younger deformational event (Fig. 4D). The southern shear zone developed in the Lipetrén superunit (site P20 in Table S3 [see footnote 1]; Figs. 4E–4H) is ~20 m thick. It consists of fine-grained pink mylonitic rocks with a regular ~N-S, subvertical foliation. A moderately to steeply plunging lineation is defined by elongated quartz and feldspars. von Gosen and Loske (2004) described uplift of the western block with a sinistral component. The two ductile shear zones that crop out

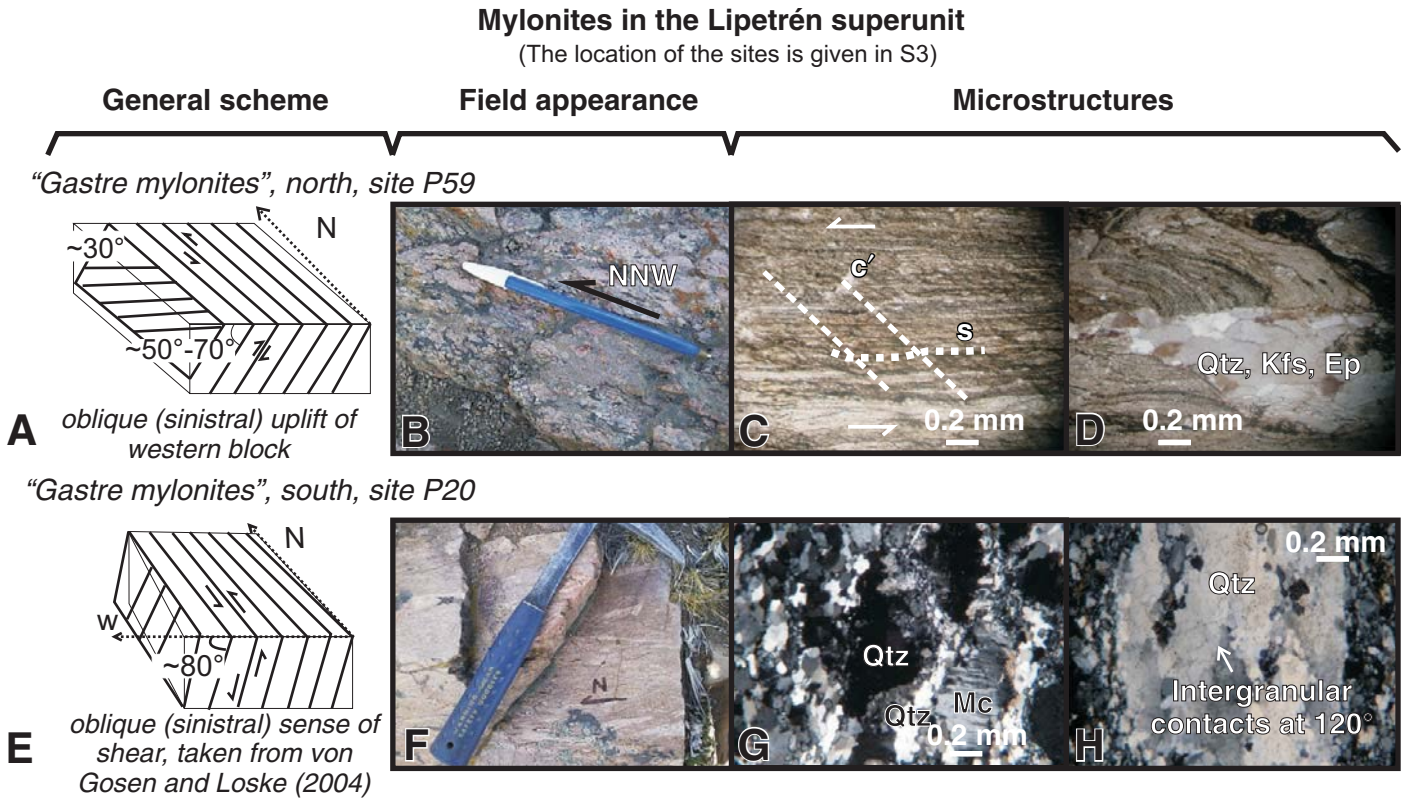

Figure 4. Mylonites in the Lipetrén superunit; their location can be found in Table S3 (see footnote 1). (A)–(D) General scheme, field appearance, and microstructures of the northern strip of mylonites east of Gastre town at site P59. (A) General scheme of the "Gastre mylonites" of von Gosen and Loske (2004) with a NNW-SSE strike, steeply dipping to the W-SW, and with an oblique (sinistral) sense of shear. (B) Thin foliation planes of NNW-SSE strike. (C) S-C′ structure defining a sinistral sense of shear; the S surfaces are defined by quartz, feldspars, micas, and opaque minerals, and they are crenulated by the C′ surfaces defined by micas. (D) Late quartz-feldspathic veins disrupting the mylonitic foliation. (E)–(H) General scheme, field appearance, and microstructures of the southern strip of mylonites east of Gastre town at site P20. (E) General scheme of the southern band of Gastre mylonites of site P20, with steeply dipping N-S foliation and a steeply plunging lineation; the dextral sense of shear is taken from von Gosen and Loske (2004). (F) Parallel foliation planes of N-S orientation. (G)–(H) Quartz and feldspar porphyroclasts surrounded by quartz and feldspar recrystallized subgrains with post-kinematic annealing. All photomicrographs were taken under crossed polars. Mineral abbreviations in all figures are after Kretz (1983). Qtz—quartz; Kfs—K-feldspar; Ep—epidote; Mc—microcline.

east of the Gastre village show triple junctions among quartz and feldspars, suggesting that they were overprinted by late to post-kinematic annealing.

ANISOTROPY OF MAGNETIC SUSCEPTIBILITY (AMS)

Anisotropy of magnetic susceptibility (AMS) is a standard technique for petrofabric studies in granitoids (e.g., Archanjo et al., 1995, 2002; Saint Blanquat and Tikoff, 1997; Ferré and Améglio, 2000; McNulty et al., 2000; Neves et al., 2003; Žák et al., 2005; D'Eramo et al., 2006; Stevenson, 2009; Olivier et al., 2016). In particular, AMS provides a determination of the magmatic lineations, which are generally hard to measure in the field or in the laboratory. The three principal axes of the AMS ellipsoid ($K_{max} \geq K_{int} \geq K_{min}$) define a magnetic lineation parallel to K_{max} and a magnetic foliation as the plane containing K_{max} and K_{int}, with K_{min} being the pole to foliation. The common relationship between the AMS ellipsoid and petrofabric shows the magnetic lineation parallel to the structural lineation (stretching direction) and the magnetic foliation parallel to the structural foliation (flattening plane) (Borradaile and Jackson, 2010).

The low-field AMS survey in the CPB comprises a total of 149 sites (stations; 1219 oriented cores; the number of cores of each station is the "N" in Tables S1–S3 [see footnote 1]), of which 16 sites were included in previous studies (Zaffarana et al., 2010, 2012; the sites included in previous studies are shown with one or two asterisks in Tables S1–S3 [see footnote 1]). AMS measurements were performed using a MFK1-B Kappabridge susceptibilimeter. AMS ellipsoids were calculated using matrix averaging routines (Jelinek, 1978) with the programs Anisoft 4.2 (Chadima and Jelinek, 2009). The Gastre superunit was studied in 91 sites (72 bearing magmatic fabric and 19 bearing solid-state deformation fabric), and the Lipetrén superunit was studied in 52 sites (43 with magmatic fabric and nine with solid-state deformation fabric). The host rock was studied in six sites.

Determining the minerals that dominate the magnetic signal is important when analyzing AMS data. To do this, we performed hysteresis curves and isothermal remanent magnetization-backfield analyses in order to gain information on coercive force H_c, saturation magnetization M_s, remanent magnetization M_r, and remanent coercive force H_{cr}, which allow estimating the domain state (i.e., size) of titanomagnetites. Temperature variation of bulk magnetic susceptibility (thermomagnetic curves) was also applied to further investigate the magnetic properties of rock minerals (e.g., Hrouda, 2003, 2010). Additionally, representative specimens were studied via performing thermomagnetic curves and inspection of polished sections in order to gain further insights into oxide mineralogy.

MAGNETIC MINERALOGY

The degree of magnetization of a material in response to an applied magnetic field is reflected by a dimensionless proportionality constant known as magnetic susceptibility (K). The bulk or mean magnetic susceptibility of a rock reflects the sum of the individual contributions from all of its forming minerals ($K_m = [K_{max} + K_{int} + K_{min}] / 3$), so magnetic susceptibility has compositional significance. Bouchez (2000) proposed that when bulk magnetic susceptibility is higher than 4×10^{-4} SI, the magnetic susceptibility is mainly controlled by ferromagnetic minerals (mainly magnetite), and the rock can be classified as "ferromagnetic". In contrast, when bulk magnetic susceptibility is lower than this value, it is assumed to be largely controlled by paramagnetic minerals (e.g., mafic silicates), and the rock can be classified as "paramagnetic". In the Lipetrén superunit, there are sites whose mean bulk susceptibility is on the order of 10^{-5} SI, therefore they are classified as weakly paramagnetic. The classification of each AMS site is given in Tables S1–S3 (see footnote 1). In Figures S1–S4 (see footnote 1), there are also detailed descriptions of the magnetic mineralogy of each unit.

The distribution of K_m shows that sites with $K_m < 1 \times 10^{-3}$ SI predominate (Fig. 5A), because even though there is compositional variation between granites and diorites, the acidic terms (granites and granodiorites) predominate. Mean magnetic susceptibility in the Gastre superunit is 19.45×10^{-3} SI, so it is comprised by ferromagnetic granites (Bouchez, 2000). Titanomagnetite is in all cases the main ferromagnetic mineral in the Gastre superunit, appearing as isolated grains included in other minerals or forming part of biotite + amphibole clusters. In general, higher values of K_m correlate with higher contents of mafic minerals in the Gastre superunit (the hornblende quartz diorites tend to show the greatest K_m values; see the correlation in K_m in Fig. 5A and the composition patterns within the CPB shown in Fig. 1).

In the Lipetrén superunit, opaque minerals are <1% in volume and are generally present as isolated euhedral to subhedral grains that occur as inclusions in other minerals. A second generation of anhedral opaque minerals is present along biotite cleavage planes and is interpreted to be associated with the alteration of biotite. Average mean magnetic susceptibility for the monzo- and syenogranites of this superunit is 2.95×10^{-3} SI. According to their susceptibility value, 30 sites of the biotitic granites of the Lipetrén superunit have been classified as ferromagnetic, eight sites as paramagnetic, and seven sites as weakly paramagnetic (these biotitic granites appear as sites with $K_m < 1 \times 10^{-3}$ SI in Fig. 5A). Hematite is also present in some cases within the opaque phases of the biotitic granites of the Lipetrén superunit as deuteric alteration of biotite and titanomagnetite (see Supplemental Figure S4 [see footnote 1]). Magnetic susceptibility of the Horqueta Granodiorite is rather homogeneous, around 37×10^{-3} SI, and dominated by multidomain (MD) magnetite (these sites are included in the group with $<1 \times 10^{-3}$ SI in Fig. 5A).

The Calcatapul Formation is largely dominated by MD magnetite (Zaffarana et al., 2010). Mean susceptibility values from the Yancamil Granite (1.8×10^{-3} SI; Table S1 [see footnote 1]) are compatible with the ferromagnetic field, however hysteresis loops and the thermomagnetic curves from this unit show that its magnetic susceptibility is actually controlled by the superimposed effects of both magnetite and paramagnetic minerals.

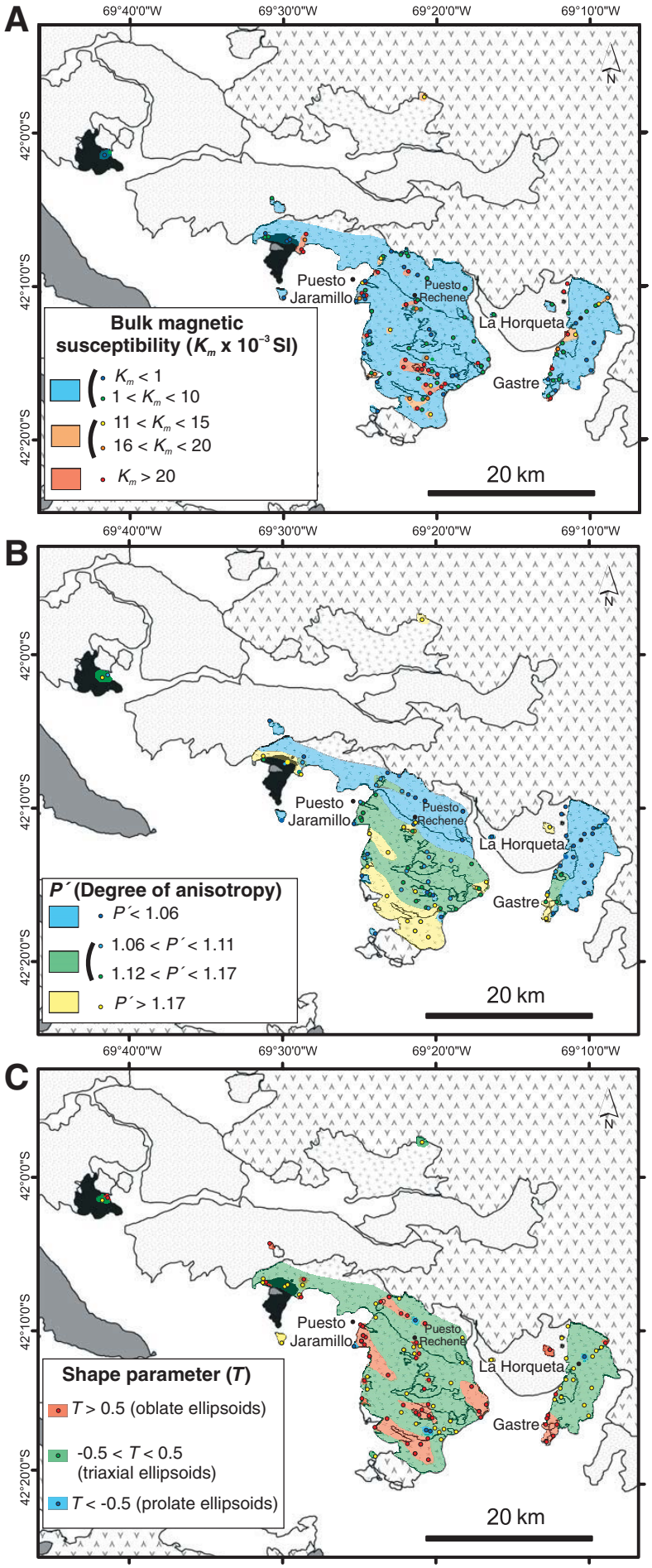

Figure 5. Hand-contoured map of various parameters in the Central Patagonian batholith. The raw data for all three maps are in Tables S1–S3 in the Supplemental Materials (see footnote 1). (A) Map of the mean magnetic susceptibility (K_m). Values are represented as K_m × 10^{-3} SI units. Note the correlation between K_m and composition patterns within the pluton (Fig. 1). (B) Map of the degree of anisotropy (*P′*). *P′* value of 1.10 represents 10% of anisotropy. (C) Map showing the shape parameter (*T*). Lithologic symbols in the maps are the same as in Figure 2I.

AMS SCALAR DATA

The degree of anisotropy of the AMS ellipsoid can be described by the corrected anisotropy degree *P′* (Jelinek 1981), which is a measure of the degree to which the AMS ellipsoid deviates from a sphere. The shape of the AMS ellipsoid can vary from oblate (pancake shaped) to prolate (pencil shaped). The *T* parameter, where $T = (\ln F - \ln L) / (\ln F + \ln L)$ (Jelinek 1981) is one way of describing the ellipsoid shape, where *L* is the magnetic lineation (K_{max} / K_{min}) and *F* is the magnetic foliation (K_{int} / K_{min}). The magnetic ellipsoid is oblate for $0 \le T \le 1$ and prolate for $-1 \le T \le 0$.

In general, in both in the Gastre and Lipetrén superunits of the CPB there seems to be a weak correlation between K_m and *P′*, suggesting that there could be some compositional (magnetite content) control on rock anisotropy (Fig. 6A). This is also reflected in the maps, as the sites with higher K_m generally have higher anisotropy degree (Figs. 5A–5C). However, beyond this weak compositional control in the anisotropy, the magmatic fabrics of both superunits show a direct relationship between anisotropy degree *P′* and *T*, as more anisotropic fabrics are more strongly oblate (higher T; Figs. 5B–5C). In the maps, the highest anisotropy degree values (P′ > 6%) are found in the region between Gastre and Puesto Jaramillo (Fig. 5B). This is also the area where the magmatic (magnetic) foliations of the CPB define a well-ordered NW-SE–striking, steeply dipping pattern (see the next section). In addition, this area tends to concentrate the most strongly oblate magmatic fabrics (T > 0.5; Fig. 5C; compare with the fabric types of Fig. 2I). The anisotropy degree is lower (<6%) toward the north of Puesto Rechene and also in the area between Gastre and La Horqueta (Fig. 5B), where more disordered magmatic fabrics are seen (see the next section). Prolate ellipsoids (with T > 0.5) are very scarce and their location is random (Fig. 5C).

With respect to overprinting of solid-state deformation on the magmatic fabrics, the behavior is slightly different in each superunit. In the Gastre superunit, granites that underwent low-temperature solid-state deformation have lower mean susceptibility values than rocks having exclusively magmatic petrofabric. This could be explained by magnetite alteration to hematite by fluid circulation during low-temperature deformation. An exception to this behavior is the dioritic dikes of the hornblende quartz diorites, which show a slight increase of *P′* associated with higher values of K_m. This case could be explained, instead, by magnetite generation due to biotite alteration during low-temperature deformation. In the Lipetrén superunit, *P′* values >10% are nearly everywhere seen in rocks with overprinting of magmatic fabrics by low-temperature solid-state deformation (Figs. 6A–6B), suggesting that during solid-state deformation there is magnetite generation in these rocks. With respect to the shape of the AMS ellipsoids, in the sites where the magmatic fabric is overprinted by low-temperature solid-state deformation, oblate ellipsoids (*T* > 0.5) predominate (Fig. 6B).

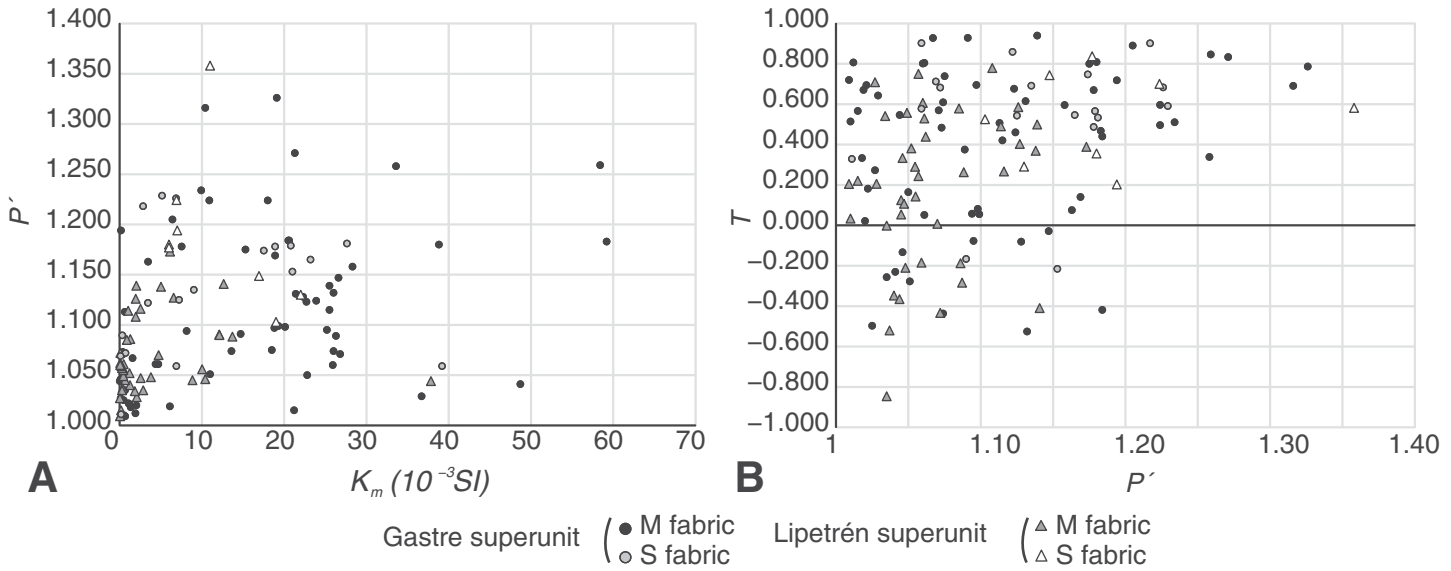

Figure 6. Anisotropy of magnetic susceptibility scalar data in the sites of the Central Patagonian batholith with magmatic (M) and solid-state (S) fabrics. (A) *P′* versus K_m. (B) *T* versus *P′*. *P′*—corrected anisotropy degree (Jelinek, 1981); K_m—mean susceptibility; *T*—shape parameter of the magnetic fabrics (Jelinek, 1981).

AMS DIRECTIONAL DATA

In all cases where measurement of magmatic or tectonic foliations was possible in the field, we noted that they are parallel to the corresponding magnetic foliation. Parallelism between the visible lineation and the magnetic lineation in areas of solid-state deformation was also observed, also including the two localities of the Calcatapul Formation. Coaxiality between magmatic-tectonic and magnetic fabrics is independent of the mineral that dominates the bulk susceptibility of the rock. These observations strongly suggest that the magnetic fabric of the rocks appropriately represents their petrofabric and is a suitable tool to map the internal structure of the plutons.

Overall, the magnetic fabrics show roughly coherent patterns throughout the studied area. The more conspicuous feature in the internal structure of the studied granitoids is the presence of NW-SE–trending, dominantly steeply dipping magmatic (magnetic) foliations in the rocks of the Gastre superunit, especially in the Loma Alta area (between Gastre and Puesto Jaramillo; Fig. 7; Table S2 [see footnote 1]). These NW-SE subvertical magmatic foliations are parallel to slightly oblique with respect to the contacts among units (Fig. 7). The four AMS sites belonging to enclave swarms hosted by the porphyritic biotite-hornblende monzogranites of the Gastre superunit also comprise subvertical NW-SE magmatic foliations in this area (sites marked with an ellipse in Fig. 7 and individualized with stars in Fig. 8). Enclave swarms can be considered as the trace of feeder conduits (Tobisch et al., 1997; Collins et al., 2006) in the CPB. Local deviations of the general subvertical NW-SE trend exist where the contacts of the units of the Gastre superunit display irregular geometry and also toward the north of Puesto Rechene (northern Loma Alta area; see Fig. 7), where the granites of the Gastre superunit also have N-S to NNE-SSW steeply to moderately dipping magmatic (magnetic) foliations (Fig. 8).

Similarly, the magmatic fabrics of the Lipetrén superunit are predominantly parallel to the magmatic fabrics of the Gastre superunit in the Loma Alta area (Fig. 7). However, the magmatic foliations of the Lipetrén superunit deviate from the main NW-SE subvertical trend defined by the magmatic fabrics of the Gastre superunit in the Puesto Jaramillo area (see circled area in Fig. 7). Furthermore, the morphology of the stocks of the Lipetrén superunit in the Loma Alta area is slightly more equidimensional than that of the plutons of the Gastre superunit, which have a more elongated shape. In the area between Gastre and La. Horqueta (Cordón de la Cruz; Fig. 7), the magmatic (magnetic) foliations of the Lipetrén superunit display a disordered pattern, with variable strike and intermediate dip (Fig. 7). The more random magmatic (magnetic) fabrics of the Lipetrén superunit are reflected in the K_{min} orientation distribution of Figure 7.

The Gastre superunit has predominant magnetic (magmatic) lineations of alternating steep or shallow plunge, although intermediate plunges are also observed (Fig. 8). In the Puesto Jaramillo area, NW-SE shallow magmatic (magnetic) lineations are observed in the Gastre superunit (Fig. 8). In the Lipetrén superunit, the magmatic lineations can be shallowly, intermediately, or steeply plunging (Fig. 8). At La Horqueta, the magmatic (magnetic) lineations of the Lipetrén superunit are predominantly shallowly plunging (Fig. 8).

Solid-state magnetic foliations of the Gastre superunit are nearly everywhere roughly parallel to the fabrics developed in the magmatic stage (Fig. 7). Note that, unlike the magmatic fabrics, the solid-state fabrics in the Lipetrén superunit are parallel to the dominant NW-SE subvertical trend displayed by the Gastre superunit both in magmatic and in solid-state conditions (see circled area near Puesto Jaramillo in Fig. 7). The solid-state lineations in the Gastre and Lipetrén superunits can show either high, intermediate, or shallow plunge, although steeply plunging lineations predominate in both superunits (Fig. 8; Table S3 [see footnote 1]).

DISCUSSION

Emplacement Depth of the CPB: Adjoining Plutons Emplaced at Different Crustal Levels

Equilibrium crystallization pressures for the Gastre superunit determined from amphibole compositions by Zaffarana et al. (2014) are reevaluated here in light of the numerous problems that have been noted with the Al content in hornblende as a geobarometer (i.e., Erdmann et al., 2014). One important problem is that the total Al content in amphibole results not only from the pressure-dependent tschermakitic substitution but also from the temperature-dependent edenitic substitution (Erdmann et al., 2014). To infer more real emplacement pressures, we followed the approach of Ribeiro et al. (2016), which consists of comparing the composition of the amphiboles of the Gastre superunit (reported in Zaffarana et al., 2014) with the compositions of experimental amphiboles crystallized under different pressure conditions (e.g., Samaniego et al., 2010). Crystallization and melting experiments show that the Al^T (total aluminum content), Mg≠ (magnesium number; Mg#=100 × mol.Mg/(mol.MgO+mol.FeO)), and Na + K contents of amphiboles vary with pressure and temperature, and that their compositions plot within distinct pressure-dependent compositional fields (Scaillet and Evans, 1999; Prouteau and Scaillet, 2003; Alonso-Perez et al., 2009). The comparison of the amphiboles of the Gastre superunit with those compositional fields demonstrates a good fit for the field of 2.2 kbars (Supplemental Figure S5 [see footnote 1]), and therefore the emplacement depth of the Gastre superunit is consistent with shallow crustal levels, mostly between 6 and 7 km.

Likewise, the presence of miarolitic cavities and microgranophyric textures in the Lipetrén superunit (Zaffarana et al., 2014) supports the conclusion that it was emplaced in a shallower subvolcanic environment, under pressures of probably <1.5–1.2 kbar (Candela, 1997). Overall, isotopic, geobarometric, and field data document that the Gastre area underwent 3–4 km of exhumation during a time span of ~7 m.y. in the Late Triassic. Consequently, the CPB comprises adjoining plutons crystallized at slightly different crustal depths (3–4 km

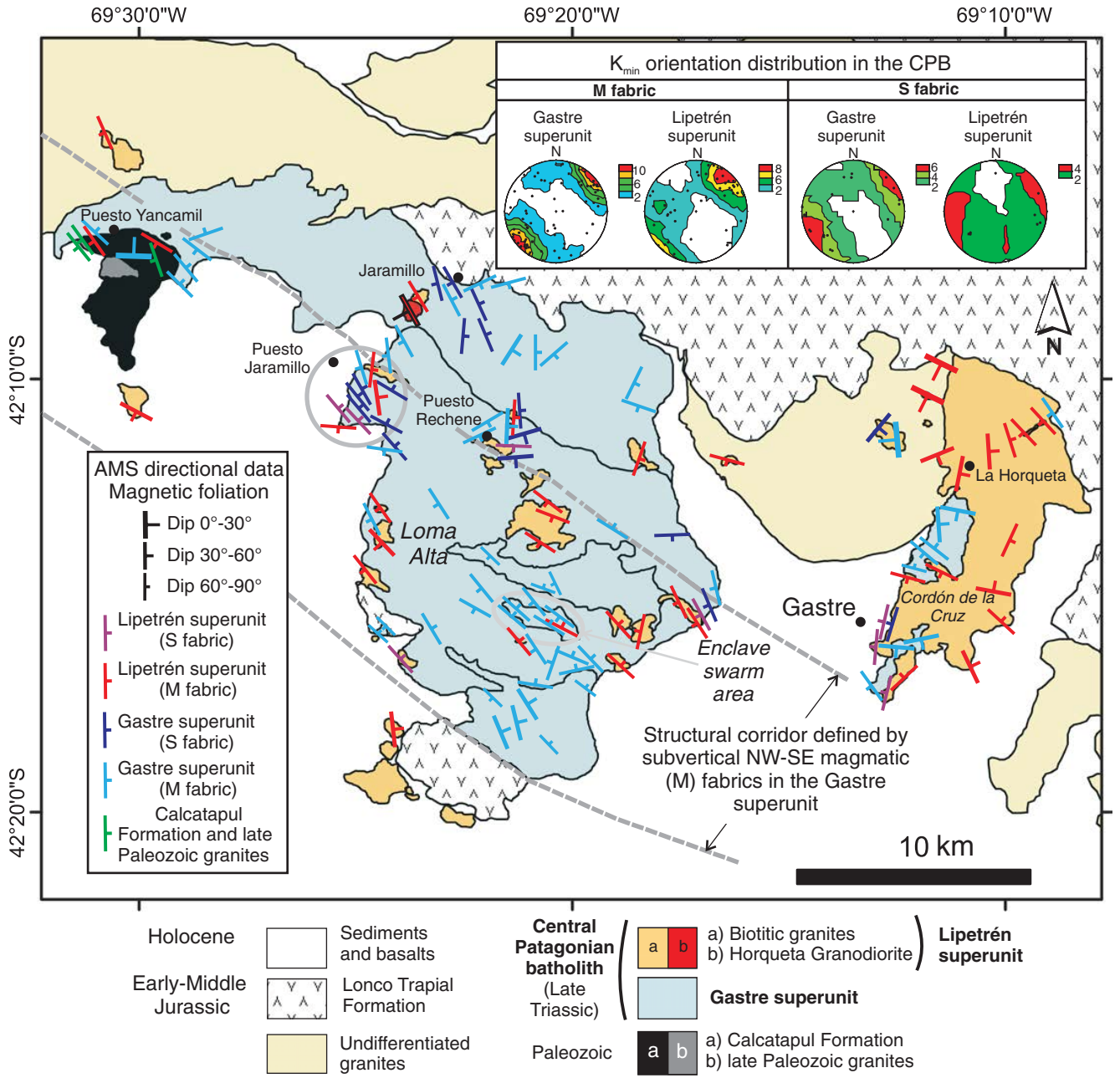

Figure 7. Map showing magnetic foliation planes (K_{max}-K_{int} planes), defined as the plane perpendicular to K_{min}, in the Central Patagonian batholith (CPB). The dashed lines represent the Gastre corridor of magmatic fabrics, whose strike was defined only with those magnetic fabrics of high inclinations (from 60° to 90°). The circle around Puesto Jaramillo encloses the area where the magmatic fabrics of the Lipetrén superunit are not parallel to the magmatic and solid-state fabrics of the Gastre superunit. In contrast, the solid-state fabrics of the Lipetrén superunit are parallel to the magmatic and solid-state fabrics of the Gastre superunit. Inset shows K_{min} distribution of the magmatic (M) and low-temperature solid-state (S) fabrics (as described in the field) within the Gastre and Lipetrén superunits. The stereonets represent Kamb contoured equal-area lower-hemisphere stereographic projections made with the software Stereonet 9.9.5 (Allmendinger et al., 2013; Cardozo and Allmendinger, 2013). The scale represents Kamb contours in standard deviation. AMS—anisotropy of magnetic susceptibility.

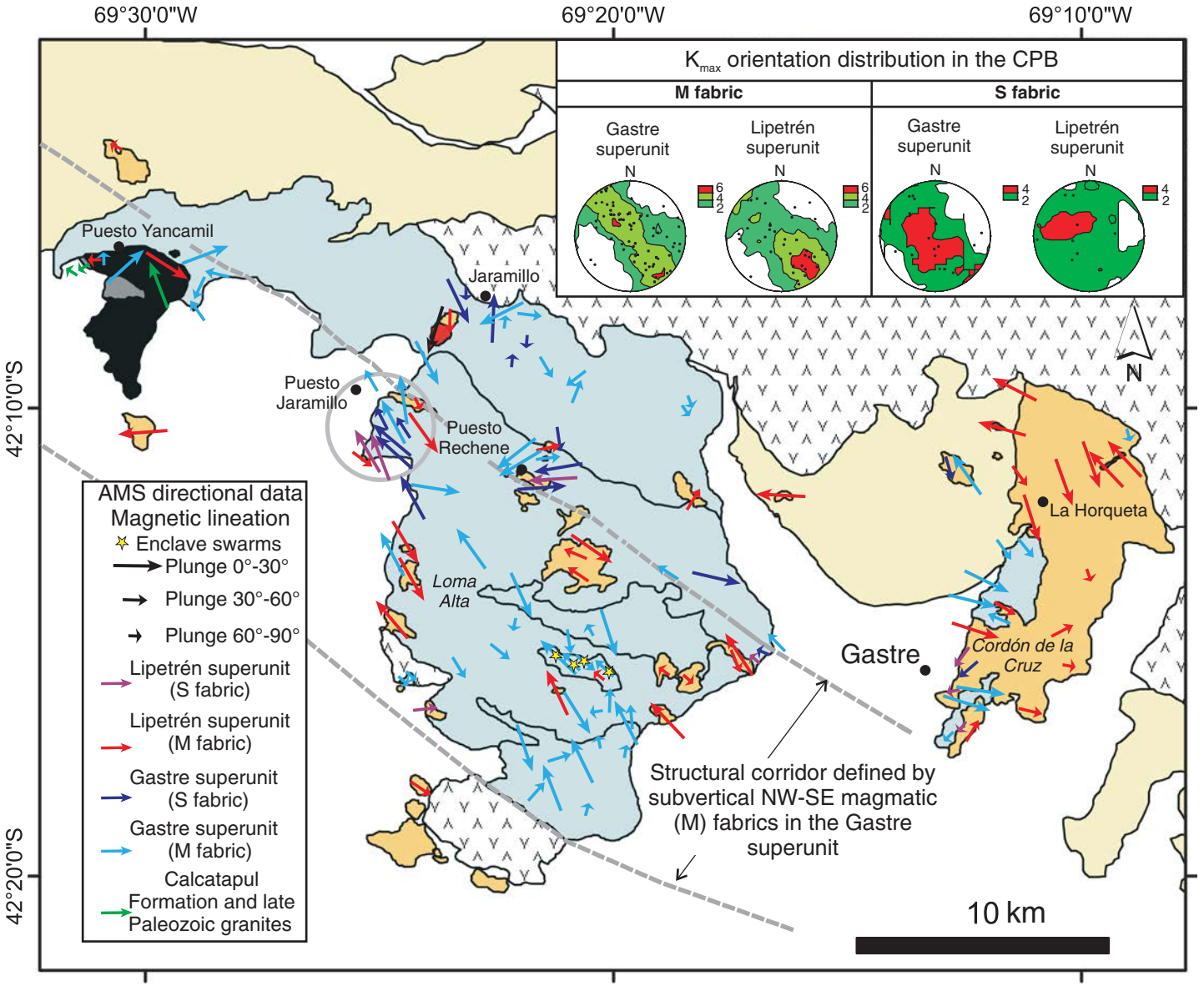

Figure 8. Map showing magnetic lineation (K_{max} direction) in the Central Patagonian batholith (CPB). The dashed lines represent the Gastre corridor of magmatic fabrics, whose strike was defined only with those magnetic fabrics of high inclinations (from 60° to 90°). As in Figure 7, the circle shows the area where the fabrics of the Lipetrén superunit bear a different strike with respect to the magmatic and solid-state fabrics of the Gastre superunit. Inset shows K_{max} distribution of the magmatic (M) and low-temperature solid-state (S) fabrics (as described in the field) within the Gastre and Lipetrén superunits. The stereonets represent Kamb contoured equal-area lower-hemisphere stereographic projections made with the software Stereonet 9.9.5 (Allmendinger et al., 2013; Cardozo and Allmendinger 2013). The scale represents Kamb contours in standard deviation. Lithologic symbol explanations as in Figure 7. AMS—anisotropy of magnetic susceptibility.

of vertical distance). These different crustal depths may have influenced the emplacement mechanisms of the two magmatic suites.

Internal Structure of the CPB: Magma Emplacement and Pluton Construction by Amalgamation of Dike-Like Bodies in a Transpressive Regime

Most of the rocks of the CPB have magmatic fabrics with triaxial to oblate ellipsoids. The most outstanding characteristic when analyzing the magmatic foliations of the Gastre superunit is the presence of a structural corridor of predominantly subvertical NW-SE orientation (Fig. 7). The magmatic foliations can be slightly oblique with respect to the NW-SE trend of the contacts among the units of the Gastre superunit. The plunge of magnetic lineation in the magmatic fabrics of the Gastre superunit varies from steep to shallow (Fig. 8). The magmatic lineation is interpreted as the direction of stretching. In the areas where the magnetic ellipsoids of the Gastre superunit are triaxial, and therefore their magnetic lineation is well defined (Fig. 5C), we find steeply, intermediately, and shallowly plunging lineations interspersed (Fig. 8).

AMS data combined with gravimetric surveys commonly lead to discovery of a granite root or feeder zones (Vigneresse, 1995; Vigneresse and Bouchez, 1997). However, enclave swarms, which are places where mafic and felsic magmas interact, leading to highly heterogeneous rocks, have also been interpreted as possible batholith root zones (Tobisch et al., 1997; Moyen et al., 2003; Collins et al., 2006). The tabular enclave swarms hosted by the porphyritic biotite-hornblende monzogranites of the Gastre superunit could represent root zones within the CPB, and they also bear the predominantly subvertical magmatic NW-SE fabrics (Fig. 7). There, the AMS ellipsoids are strongly oblate, and therefore their intermediately to shallowly plunging magnetic lineation is not so well defined compared to triaxial or prolate sites (Fig. 5C).

The magmatic foliations of the stocks of the Lipetrén superunit are predominantly parallel to those of the Gastre superunit (Fig. 7), but near Puesto Jaramillo the magmatic foliations of the Lipetrén superunit are strongly discordant to the general trend of the batholith (see circled area in Fig. 7). In addition, in the area between Gastre and La Horqueta, the magmatic foliations of the Lipetrén superunit display variable strike and are of intermediate dip in a disordered pattern (Fig. 7). The magnetic lineations (in predominantly triaxial magnetic ellipsoids) are of variable plunge (Figs. 6C, 8). The shallow foliations of the Lipetrén superunit in the area around La Horqueta may correspond to structurally higher emplacement levels, where magma sheets flowed parallel to the roof of the pluton (Fig. 7). In addition, west of Puesto Uribe, von Gosen and Loske (2004) observed that undeformed porphyries of Lipetrén biotitic granites intrude foliated granodiorites ascribed to the Gastre superunit, suggesting that the deformation that controlled the emplacement of the Gastre superunit would not have lasted throughout the emplacement of the Lipetrén superunit.

Several observations throughout the CPB would suggest that it was emplaced by the amalgamation of dike-like magma bodies. For instance, the biotitic granites of the Lipetrén superunit in the area of La Horqueta intrude the equigranular hornblende-biotite granodiorites of the Gastre superunit, forming tabular bodies (Zaffarana et al., 2014, their figure 7A). In addition, the magmatic dikes of the CPB that intrude the NW-SE–foliated Calcatapul Formation at Estancia Yancamil (von Gosen and Loske, 2004) constitute another piece of evidence for dike emplacement. Our paleomagnetic information (work in progress) indicates that outcrops of the CPB having remanence of normal polarity are interspersed with those carrying reversed-polarity magnetization, therefore suggesting that the CPB is formed by multiple plutonic units which were injected episodically, cooling through the blocking temperatures.

Within the CPB, the granites with low-temperature solid-state deformation of the Gastre and Lipetrén superunits predominantly bear NW-SE subvertical foliation planes (Fig. 7), suggesting that the deformation that controlled the magmatic fabrics of the Gastre superunit continued to operate during cooling of both intrusive suites. The lineations of the tectonically deformed granites are either subhorizontal (as in the area of Puesto Jaramillo; Fig. 8) or subvertical (toward the west of Gastre village; Fig. 8). The magnetic ellipsoids of the low-temperature deformed rocks are mostly oblate, but the direction of the tectonic lineation was in all cases observed in the field as well. The presence of magmatic and solid-state vertical, intermediate, and horizontal lineations, together with the predominance of subvertical oblate ellipsoids (Figs. 6C, 7, 8), would suggest that the emplacement of the CPB would have taken place within a transpressive strike-slip zone with partition of the deformation (Fossen et al., 1994; Tikoff and Greene, 1997; Fossen and Tikoff, 1998; Saint Blanquat et al., 1998). Transpressive environments are rather common in magmatic arcs in conditions of slightly oblique convergence (Saint Blanquat et al., 1998). In this context, the less-controlled general morphology and magmatic fabrics of the Lipetrén superunit can be ascribed to its shallower emplacement level compared to the Gastre superunit, which would make it less affected by transpression-induced forces (Saint Blanquat et al., 1998). The exhumation of the CPB was coeval with the development of metamorphic accretionary complexes in the Patagonian Andes (Thomson and Hervé, 2002; Hervé et al., 2003, 2008), as well as with the Peninsula orogeny in West Antarctica (Miller, 1983; Vaughan and Livermore, 2005) and with the Rangitata I orogeny in New Zealand (Bradshaw et al., 1981; Vaughan and Livermore, 2005). This supports the concept that the uplift and denudation of the CPB was associated with an accretionary episode of regional extent along the proto-Pacific margin of Gondwana.

The shallower emplacement level of the Lipetrén superunit (~3 km or less) would allow roof uplift as one of the possible space-making processes that could have helped the intrusion of stocks. The Gastre superunit has more rectilinear fabric, as is normal in deeper zones within batholiths emplaced in transcurrent environments (Moyen et al., 2003).

Structural observations in the mylonite-hosting Calcatapul Formation at Puesto Yancamil have led several workers to propose a predominantly sinistral shear component (Franzese and Martino, 1998; von Gosen and Loske, 2004;

Zaffarana et al., 2010). Moreover, Zaffarana et al. (2010) proposed that transpressive deformation controlled the syntectonic emplacement of the late Paleozoic Yancamil Granite. If the Uribe mylonite (Fig. 3A), which is the thickest mylonite zone within the domain of the CPB, effectively represents a mylonitized granite of the Gastre superunit, then this would be strong evidence of the syntectonic emplacement of the Gastre superunit within a sinistral transpressive regime. This deformation would have lasted from late Paleozoic to Early Triassic times. The Rechene mylonite has sinistral sense of shear, thus its kinematics is concordant with that of the Uribe mylonite. The Horqueta mylonite and the S-C mylonite at site P144 (Figs. 3I–3M) display kinematic indicators of dextral motion, but they have a different trend than the rest of the batholith. Possible dextral solid-state strike-slip motion has been also noted by von Gosen and Loske (2004) in the area of Jaramillo (Fig. 1). These authors also reported a conjugate set of subvertical, dextral and sinistral shear planes affecting Paleozoic rocks and CPB granites at Estancia Yancamil, interpreting this younger deformation as a response to post-CPB NE-SW compression. Finally, the mylonites found at the east of Gastre have a sinistral shear sense component (Figs. 4A–3H), but their tectonic foliation is not parallel with the magmatic fabrics in the same area (Fig. 7). Curiously, the N-S orientation of these mylonitic bands is parallel to the trend of the valley that connects Gastre with La Horqueta (Fig. 7), suggesting that they could have been produced by a younger structure, probably Andean, which could be responsible for the uplift of the Cordón de la Cruz.

Tectonic Model for the Emplacement of the CPB

Having analyzed the magmatic and tectonic fabrics of the CPB and their possible significance, we interpret that the CPB emplaced syntectonically within a sinistral transpressive system (Fig. 9). At stage 1, the intrusion of the earliest facies of the Gastre superunit took place in a dominantly NNW-SSE– to NW-SE–elongated crustal deformation zone (Fig. 9A). In this sense, the NNW-SSE subvertical magmatic foliations and the steeply dipping lineations of the porphyritic biotite-hornblende monzogranites of the Gastre superunit located north of Puesto Rechene area (Figs. 7–8) could represent early-formed magmatic fabrics. At stage 2, the intrusion zone enlarged during the injection of the main facies of the Gastre superunit: the equigranular biotitic monzogranites, the equigranular hornblende-biotite granodiorites, and the porphyritic biotite-hornblende monzogranites hosting the enclave swarms (Fig. 9B). In this tectonic framework, the subvertical NE-SW orientation is an extensional direction, and it coincides with the predominant orientation of the dioritic to quartz-dioritic dikes of the Gastre superunit. Finally, the more isotropic biotitic granites of the Lipetrén superunit intruded at shallower crustal levels during the exhumation of the Gastre superunit (stage 3 in Fig. 9C).

Note that the fabric observed in the CPB roughly matches the structural grain of northern Patagonia, which has a predominant NW-SE subvertical orientation that has been likely inherited from the pervasive late Paleozoic deformation (von Gosen, 2002, 2003, 2009; Álvarez et al., 2014; Giacosa et al., 2004, 2014, 2017). A similar geometry is seen in other Triassic plutons from northern Patagonia cropping out as far as 300 km north of the CPB, where a NW-SE–trending subvertical fabric, including mylonites, has been observed (e.g., Báez et al., 2016). This crustal structure in northern Patagonia also played a role in controlling the opening of the Jurassic basins during the early stages of the Andean tectonic cycle (e.g., Figari et al., 1994, 2015). Considering these observations, the magma batches that form the CPB could have been emplaced along preexisting fractures, within a previously structured upper crust (e.g., as in Fig. 9). This has been recognized in other localities of northern Patagonia, where a previously acquired crustal structure channeled early Mesozoic igneous intrusions (e.g., Márquez et al., 2011; González et al., 2014).

We envisage that the model depicted in Figure 9 is strongly dependent on the inferred Late Triassic age of the oblique-sinistral mylonites at Puesto Uribe. If the deformation of those mylonites with granitic protolith (Uribe mylonite; Fig. 3A) were of late Paleozoic age (as happens with the late Paleozoic Yancamil Granite, which was deformed in late Paleozoic times as stated by von Gosen and Loske [2004]), then there would not be enough arguments to propose that the same sinistral transpressive deformation lasted protractedly throughout the emplacement of the CPB. Nonetheless, the CPB does show evidence for transpressive deformation, but it could have been produced by a separate event in the Early Triassic whose kinematics would not be clear in light of the present data. However, the results of this study contradict the hypothesis that the CPB has been affected by continental-scale Jurassic dextral shearing through the Gastre fault system. This conclusion arises for three reasons: (1) mylonites with sinistral shear sense predominate in the host rock of the CPB, (2) the mylonite zones that traverse the granitic rocks in the area of Gastre are generally thin, and (3) the NW-SE and NNW-SSE mylonite zones with suspected CPB protoliths (including Uribe mylonite, which is the thickest one) record a sinistral shear sense component (Figs. 3, 4).

Implications for the Kinematics and Timing of Deformation of the Gastre Fault System

The sinistral transpressive syntectonic emplacement of CPB probably took advantage of a preexisting fabric within the structural grain of northern Patagonia, and this conclusion has further implications for the existence of the NW-SE subvertical Gastre fault system. The CPB is located in the type locality of this controversial fault, and its outcrops have been considered as records of the activity of the Gastre fault system (Rapela et al., 1991, 1992; Rapela and Pankhurst, 1992). Figure 1A shows the inferred trace of the Gastre fault system passing along the outcrops of the Late Triassic CPB. Recent paleomagnetic data from the overlying Lonco Trapial Formation (Fig. 1B) signal that no clockwise tectonic rotations took place in the Jurassic throughout the Gastre district (Zaffarana and Somoza, 2012). Other arguments coming from regional geological observations can be used against the postulated Jurassic strike-slip

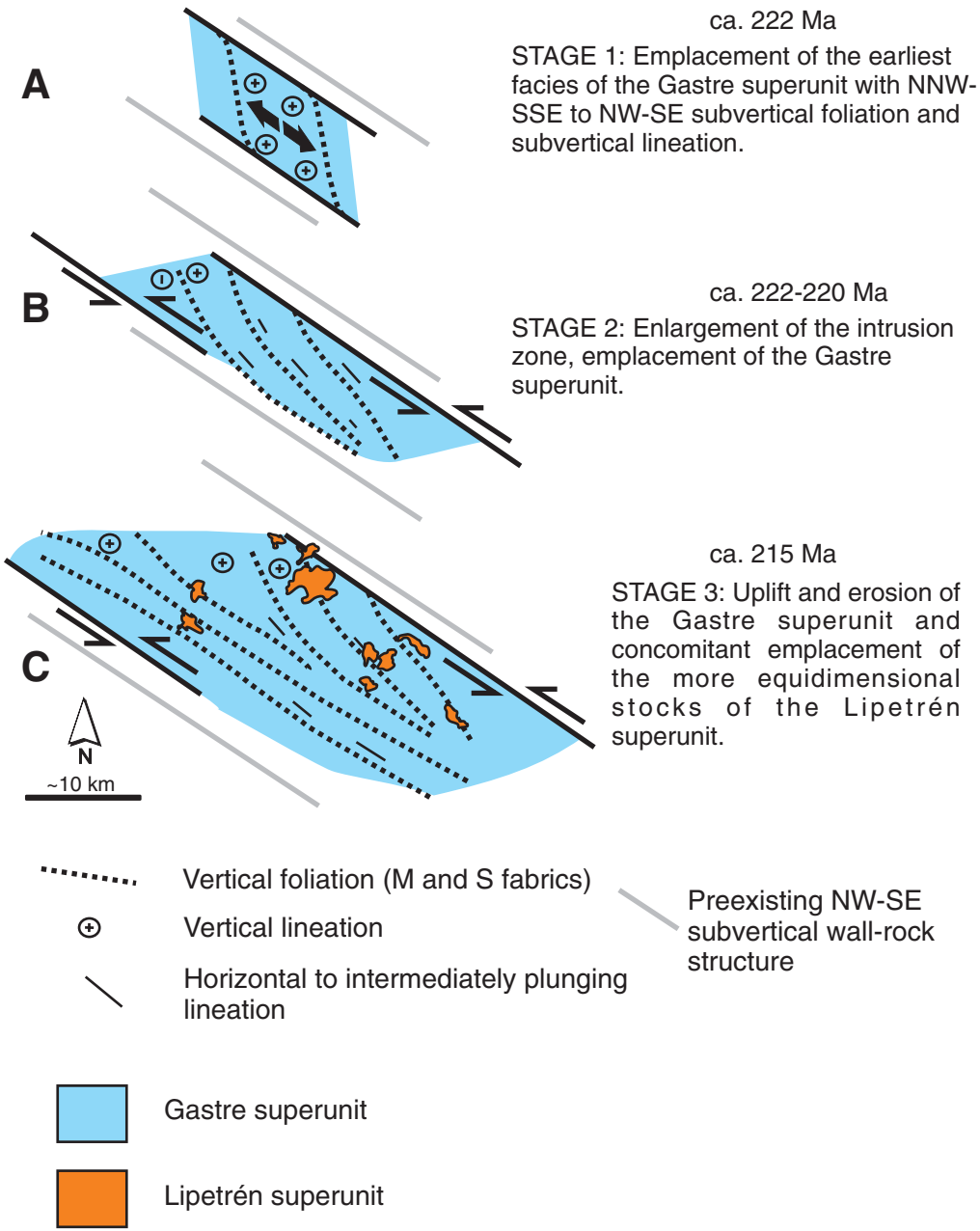

Figure 9. Simplified emplacement model of the Central Patagonian batholith based on Saint Blanquat et al. (1998). (A) The first stage of magma intrusion is NNW-SSE, at high angle with respect to the inferred regional strain orientation. (B) Tectonically assisted intrusion of the Gastre superunit. (C) Magmatic overpressuring causes emplacement of the more equidimensional stocks of the Lipetrén superunit. M fabrics—magmatic fabrics classified in the field; S fabrics—solid-state fabrics classified in the field.

motion through the Gastre fault system between northern and southern Patagonia. For example, Figure 1A shows the outcrops of the basal megasequence in the Cañadón Asfalto Basin (Figari et al., 1994, 2015), composed of the 189–183 Ma ($^{40}Ar/^{39}Ar$ on amphiboles, $^{206}Pb/^{238}U$ on zircons) Las Leoneras and Lonco Trapial Formations (Zaffarana and Somoza, 2012; Figari et al., 2015). The basal megasequence in the Cañadón Asfalto Basin overlays the Gastre fault system without discernible offset, suggesting no Jurassic strike-slip motion through this fault system. In addition, on the Chilean coast there are almost continuous exposures of Permian to Triassic metamorphic complexes (Glodny et al., 2008; Kato and Godoy, 2015) which continue across the supposed westernmost segment of the Gastre fault system without any dextral offset (only a sinistral deflection is seen at 38°S; Fig. 1A). Furthermore, the trend delineated by outcrops and borehole rocks of the fault-bounded, late Pliensbachian–Toarcian Pampa de Agnia Basin (Lesta et al., 1980; Uliana and Biddle, 1987; Uliana and Legarreta, 1999; Vicente, 2005) traverses the San Jorge Basin without any offset. Another possible major boundary between northern and southern Patagonia has been inferred to exist buried beneath the Mesozoic infill of the San Jorge Basin by Pankhurst et al. (2006) (see Fig. 1A). However, these authors assign a Carboniferous age to this suture, so it would be no longer viable to accommodate the dextral motion of the Malvinas-Falklands islands.

CONCLUSIONS

Results from structural studies and AMS measurements show that the internal structure of the CPB is dominated by a pattern of NW-SE steeply dipping magmatic foliations. This pattern is clear in the deepest-formed (~6–7 km) and oldest Gastre superunit, which is composed of NW-SE–elongated plutons. The Lipetrén superunit bears more equidimensional stocks with a more disperse magmatic fabric. This younger superunit was emplaced at a slightly shallower crustal level (~3–4 km). The solid-state deformation fabrics of both superunits are parallel to each other. The magnetic lineations of magmatic origin can be shallowly, intermediately, or steeply plunging in both superunits, whereas the tectonic lineations are predominantly either steeply or shallowly plunging (although intermediate plunges are also observed). In both suites, the predominant shape of the magnetic ellipsoid is triaxial to oblate when the fabrics are magmatic, and strongly oblate when the fabrics are tectonic. The combination of oblate ellipsoids with subvertical magmatic and tectonic foliations suggests that the emplacement of the batholith was achieved within a transpressive tectonic regime. The kinematics of this strike-slip zone would be sinistral according to the oblique (sinistral) shear sense detected in the Uribe and Rechene mylonites. The magmatic fabrics of the Lipetrén superunit are interpreted as less controlled by this regional deformation, and would be more related to chamber dynamics.

Paleomagnetic studies (work in progress) and field observations further suggest that the CPB has been constructed by the amalgamation of dike-like magma bodies. The shape of these dikes could have been locally molded against NW-SE regional structures that compose the structural grain of the North Patagonian massif, which in turn seems to be inherited from the pervasive late Paleozoic deformational fabrics. Our findings (together with regional geology data) agree with those of previous studies (von Gosen and Loske, 2004; Zaffarana and Somoza, 2012) in rejecting the hypothesis of the Gastre fault system as a major Jurassic dextral fault zone traversing the Gastre locality and crosscutting Patagonia. The application of the Gastre fault system should be abandoned in models attempting to reconstruct the western Gondwana margin. The application of the Gastre fault system should be abandoned in models attempting to reconstruct the western Gondwana margin in Jurassic times.

ACKNOWLEDGMENTS

Basil Tikoff, Werner von Gosen, and Terry Pavlis are thanked for having greatly improved earlier versions of this manuscript. Pablo Diego González and Raúl Giacosa are thanked for having helped with the interpretation of the data. Noelia Auciello and Dolores Alvarez are thanked for accompanying us in the field. Sabrina Crosta is thanked for her help with the petrographic study of opaque minerals. Flavio Sives is thanked for his help with the hysteresis cycles, IRM (isothermal remanent magnetization), and backfield curves. This contribution has been made in the frame of CONICET PIP 112-200901-00766.

We dedicate this article to Dr. Rubén Somoza. C. Zaffarana was honored with his supervision of her doctoral thesis and the mentoring of this work. He was a wonderful teacher and an amazing person. We know that, after so much work, Rubén enjoys seeing this article published from Heaven. God bless your soul.

REFERENCES CITED

Allmendinger, R.W., Cardozo, N.C., and Fisher, D., 2013, Structural Geology Algorithms: Vectors & Tensors: Cambridge, UK, Cambridge University Press, 289 p.

Alonso-Perez, R., Müntener, O., and Ulmer, P., 2009, Igneous garnet and amphibole fractionation in the roots of island arcs: Experimental constraints on andesitic liquids: Contributions to Mineralogy and Petrology, v. 157, p. 541–558, doi:10.1007/s00410-008-0351-8.

Álvarez, D., Peroni, J., Giacosa, R., Silva Nieto, D., Busteros, A., and Lagorio, S.L., 2014, Evidencias magnetométricas de las estructuras andinas y prea-andinas en Gastre y Cushamen (41° 30′–43° 00′ S, SO del Macizo Norpatagónico), *in* Proceedings, XIX Congreso Geológico Argentino, Córdoba, 2–6 June: Córdoba, Argentina: Asociación Geológica Argentina, Abstract S22-3.

Archanjo, C.J., Launeau, P., and Bouchez, J.L., 1995, Magnetic fabric vs. magnetite and biotite shape fabrics of the magnetite-bearing granite pluton of Gameleiras (Northeast Brazil): Physics of the Earth and Planetary Interiors, v. 89, p. 63–75, doi:10.1016/0031-9201(94)02997-P.

Archanjo, C.J., Trindade, R.I.F., Bouchez, J.L., and Ernesto, M., 2002, Granite fabrics and regional-scale strain partitioning in the Seridó belt (Borborema Province, NE Brazil): Tectonics, v. 21, p. 3–14, doi:10.1029/2000TC001269.

Báez, A.D., Paz, M., Pino, D., Gonzalez, P.D., Cabana, M.C., Giacosa, R., Garcia, V., and Bechis, F., 2016, Geología del sector oriental del complejo plutónico volcánico Curacó (Triásico Superior), Rio Negro: Revista de la Asociación Geológica Argentina, v. 73, p. 183–194.

Blumenfeld, P., Mainprice, D., and Bouchez, J.L., 1986, C-slip in quartz from subsolidus deformed granite: Tectonophysics, v. 127, p. 97–115, doi:10.1016/0040-1951(86)90081-8.

Borradaile, G.J., and Jackson, M., 2010, Structural geology, petrofabrics and magnetic fabrics (AMS, AARM, AIRM): Journal of Structural Geology, v. 32, p. 1519–1551, doi:10.1016/j.jsg.2009.09.006.

Bouchez, J.L., 2000, Anisotropie de susceptibilite magnetique et fabrique des granites: Comptes Rendus de l'Academie Sciences, Serie IIA: Sciences de la Terre et des Planetes, v. 330, p. 1–14, doi:10.1016/S1251-8050(00)00120-8.

Bouchez, J.L., Delas, C., Gleizes, G., Nédélec, A., and Cuney, M., 1992, Submagmatic microfractures in granites: Geology, v. 20, p. 35–38, doi:10.1130/0091-7613(1992)020<0035:SMIG>2.3.CO;2.

Bradshaw, J.D., Andrews, P.B., and Adams, C.J., 1981, Carboniferous to Cretaceous on the Pacific margin of Gondwana: The Rangitata Phase of New Zealand, *in* Cresswell, M.M., and Vella,

P., eds., Gondwana Five: Selected Papers and Abstracts of Papers Presented at the Fifth International Gondwana Symposium: Rotterdam, Balkema, p. 217–221.
Cábana, M.C., Zaffarana, C.B., Orts, D., and Somoza, R., 2017, Análisis espectral con datos ASTER de la región de Gastre, Chubut, Argentina, *in* Proceedings, XX Congreso Geológico Argentino, Tucumán, 7–11 August: San Miguel de Tucumán, Argentina: Asociacion Geologica Argentina, Abstracts (in press).
Candela, P.A., 1997, A review of shallow, ore-related granites: Textures, volatiles, and ore metals: Journal of Petrology, v. 38, p. 1619–1633, doi:10.1093/petroj/38.12.1619.
Cardozo, N., and Allmendinger, R.W., 2013, Spherical projections with OSXStereonet: Computers & Geosciences, v. 51, p. 193–205, doi:10.1016/j.cageo.2012.07.021.
Cerredo, M., and López de Luchi, M., 1998, Mamil Choique Granitoids, southwestern North Patagonian Massif, Argentina: Magmatism and metamorphism associated with a polyphasic evolution: Journal of South American Earth Sciences, v. 11, p. 499–515, doi:10.1016/S0895-9811(98)00025-X.
Chadima, M., and Jelinek, V., 2009, Anisoft 4.2, Anisotropy data browser for Windows: www.agico.com.
Cohen, K.M., Finney, S.C., Gibbard, P.L., and Fan, J.X., 2016, The ICS International Chronostratigraphic Chart: Episodes, v. 36, p. 199–204, doi:10.1111/j.1502-3931.1980.tb01026.x.
Collins, W.J., Wiebe, R.A., Healy, B., and Richards, S.W., 2006, Replenishment, crystal accumulation and floor aggradation in the megacrystic Kameruka Suite, Australia: Journal of Petrology, v. 47, p. 2073–2104, doi:10.1093/petrology/egl037.
Cruden, A.R., Tobisch, O.T., and Launeau, P., 1999, Magnetic fabric evidence for conduit-fed emplacement of a tabular intrusion: Dinkey Creek Pluton, central Sierra Nevada batholith, California: Journal of Geophysical Research, v. 104, p. 10,511–10,530, doi:10.1029/1998JB900093.
Day, R., Fuller, M., and Schmidt, V.A., 1977, Hysteresis properties of titanomagnetites: Grain-size and compositional dependence: Physics of the Earth and Planetary Interiors, v. 13, p. 260–267, doi:10.1016/0031-9201(77)90108-X.
de Saint Blanquat, M., and Tikoff, B., 1997, Development of magmatic to solid-state fabrics during syntectonic emplacement of the Mono Creek Granite, Sierra Nevada batholith, *in* Bouchez, J.L., Hutton, D.H.W. and Stephens, W.E., eds., Granite: From Segregation of Melt to Emplacement Fabrics: Petrology and Structural Geology, Volume 8: Netherlands, Springer, p. 231–252, doi:10.1007/978-94-017-1717-5_15.
de Saint Blanquat, M., Tikoff, B., Teyssier, C., and Vigneresse, J.L., 1998, Transpressional kinematics and magmatic arcs, *in* Holdsworth, R.E., Strachan, R.A. and Dewey, J.F., eds., Continental Transpressional and Transtensional Tectonics: Geological Society of London Special Publication 135, p. 327–340, doi:10.1144/GSL.SP.1998.135.01.21.
D'Eramo, F., Pinotti, L., Tubía, J.M., Vegas, N., Aranguren, A., Tejero, R., and Gomez, D., 2006, Coalescence of lateral spreading magma ascending through dykes: A mechanism to form a granite canopy (El Hongo pluton, Sierras Pampeanas, Argentina): Journal of the Geological Society, v. 163, p. 881–892, doi:10.1144/0016-764905-060.
Erdmann, S., Martel, C., Pichavant, M., and Kushnir, A., 2014, Amphibole as an archivist of magmatic crystallization conditions: Problems, potential, and implications for inferring magma storage prior to the paroxysmal 2010 eruption of Mount Merapi, Indonesia: Contributions to Mineralogy and Petrology, v. 167, 1016, doi:10.1007/s00410-014-1016-4.
Ferré, E.C., and Améglio, L., 2000, Preserved magnetic fabrics vs. annealed microstructures in the syntectonic recrystallised George granite, South Africa: Journal of Structural Geology, v. 22, p. 1199–1219, doi:10.1016/S0191-8141(00)00026-2.
Figari, E.F., Courtade, S.F., and Constantini, L.A., 1994, Estratigrafía y tectónica de los bajos de Gastre y Gan Gan: Boletín de Informaciones Petroleras, v. 40, p. 75–82.
Figari, E.G., Scasso, R.A., Cúneo, R.N., and Escapa, I., 2015, Estratigrafía y evolución geológica de la Cuenca de Cañadón Asfalto, Provincia del Chubut, Argentina: Latin American Journal of Sedimentology and Basin Analysis, v. 22, p. 135–169.
Fossen, H., and Tikoff, B., 1998, Extended models of transpression and transtension, and application to tectonic settings, *in* Holdsworth, R.E., Strachan, R.A., and Dewey, J.F., eds., Continental Transpressional and Transtensional Tectonics: Geological Society of London Special Publication 135, p. 15–33, doi:10.1144/GSL.SP.1998.135.01.02.
Fossen, H., Tikoff, B., and Teyssier, C., 1994, Strain modeling of transpressional and transtensional deformation: Norsk Geologisk Tidsskrift, v. 74, p. 134–145.
Franzese, J., and Martino, R., 1998, Aspectos cinemáticos y tectónicos de la zona de cizalla de Gastre en la Sierra de Calcatapul, Provincia de Chubut, Argentina, *in* Proceedings, X Congreso Latinoamericano de Geología y VI Congreso Nacional de Geología Económica, Buenos Aires, 8–13 November: Buenos Aires, Argentina: Asociación Geológica Argentina, Actas II, p. 3.
Gapais, D., and Barbarin, B., 1986, Quartz fabric transition in a cooling syntectonic granite (Hermitage Massif, France): Tectonophysics, v. 125, p. 357–370, doi:10.1016/0040-1951(86)90171-X.
Giacosa, R., Márquez, M., Nillni, A., Fernández, M., Fracchia, D., Parisi, C., Afonso, J., Paredes, J., and Sciutto, J., 2004, Litología y estructura del basamento ígneo-metamórfico del borde SO del Macizo Nordpatagónico al oeste del río Chico (Cushamen, Chubut, 42° 10′ S – 70° 30′ O): Revista de la Asociación Geológica Argentina, v. 59, p. 569–577.
Giacosa, R.E., Gonzalez, P.D., Silva Nieto, D., Busteros, A., Lagorio, S.L., and Rossi, A., 2014, Complejo ígneo-metamórfico Cáceres: Una nueva unidad metamórfica de alto grado en el basamento de Gastre, Macizo Nordpatagónico (Chubut), *in* Proceedings, XIX Congreso Geológico Argentino, Córdoba, 2–6 June: Córdoba, Argentina: Asociación Geológica Argentina, Abstract S21-19.
Giacosa, R., Silva Nieto, D., Busteros, A., Lagorio, S., and Hernando, I., 2017, Estructura de la región occidental del Macizo Nordpatagónico, *in* Proceedings, XX Congreso Geológico Argentino, Tucumán, 7–11 August, Abstracts: San Miguel de Tucumán, Argentina: Asociación Geológica Argentina (in press).
Glodny, J., Echtler, H., Collao, S., Ardiles, M., Burón, P., and Figueroa, O., 2008, Differential Late Paleozoic active margin evolution in South-Central Chile (37°S–40°S): The Lanalhue Fault Zone: Journal of South American Earth Sciences, v. 26, p. 397–411, doi:10.1016/j.jsames.2008.06.001.
González, S.N., Greco, G.A., González, P.D., Sato, A.M., Llambías, E.J., Varela, R., Basei, M., and Sato, A., 2014, Geología, petrografía y edad U-Pb de un enjambre longitudinal no-se de diques del Macizo Nordpatagónico oriental, Río Negro: Revista de la Asociación Geológica Argentina, v. 71, p. 174–183.
Hanmer, S., and Passchier, C., 1991, Shear-sense indicators: A review: Geological Survey of Canada Paper 90-17, 72 p., doi:10.4095/132454.
Hervé, F., Fanning, C.M., and Pankhurst, R.J., 2003, Detrital zircon age patterns and provenance of the metamorphic complexes of southern Chile: Journal of South American Earth Sciences, v. 16, p. 107–123, doi:10.1016/S0895-9811(03)00022-1.
Hervé, F., Calderón, M., and Faúndez, V., 2008, The metamorphic complexes of the Patagonian and Fuegian Andes: Geologica Acta, v. 6, p. 43–53, doi:10.1344/105.000000240.
Hirth, G., and Tullis, J., 1992, Dislocation creep regimes in quartz aggregates: Journal of Structural Geology, v. 14, p. 145–159, doi:10.1016/0191-8141(92)90053-Y.
Hole, M.J., Ellam, R.M., Macdonald, D.I.M., and Kelley, S.P., 2016, Gondwana break-up related magmatism in the Falkland Islands: Journal of the Geological Society, v. 173, p. 108–126, doi:10.1144/jgs2015-027.
Hrouda, F., 2003, Indices for numerical characterization of the alteration processes of magnetic minerals taking place during investigation of temperature variation of magnetic susceptibility: Studia Geophysica et Geodaetica, v. 47, p. 847–861, doi:10.1023/A:1026398920172.
Hrouda, F., 2010, Modelling relationship between bulk susceptibility and AMS in rocks consisting of two magnetic fractions represented by ferromagnetic and paramagnetic minerals: Implications for understanding magnetic fabrics in deformed rocks: Journal of the Geological Society of India, v. 75, p. 254–266, doi:10.1007/s12594-010-0013-0.
Jelinek, V., 1978, Statistical processing of anisotropy of magnetic susceptibility measured on groups of specimens: Studia Geophysica et Geodaetica, v. 22, p. 50–62, doi:10.1007/BF01613632.
Jelinek, V., 1981, Characterization of the magnetic fabric of rocks: Tectonophysics, v. 79, p. 63–67, doi:10.1016/0040-1951(81)90110-4.
Kato, T.T., and Godoy, E., 2015, Middle to late Triassic mélange exhumation along a pre-Andean transpressional fault system: Coastal Chile (26°–42° S): International Geology Review, v. 57, p. 606–628, doi:10.1080/00206814.2014.1002119.
König, M., and Jokat, W., 2006, The Mesozoic breakup of the Weddell Sea: Journal of Geophysical Research, v. 111, B12102, doi:10.1029/2006JB004035.
Kretz, R., 1983, Symbols for rock-forming minerals: The American Mineralogist, v. 68, p. 277–279, doi:10.1016/0016-7037(83)90220-X.
Lagorio, S., Busteros, A., Silva, D., and Giacosa, R., 2015, Nuevas edades U-Pb SHRIMP en granitoides del Batolito de la Patagonia Central, Gastre, Provincia del Chubut (República Argentina), *in* Proceedings, XIV Congreso Geológico Chileno, La Serena, 4–8 October: La Serena, Chile: Sociedad Geológica de Chile, p. 874–877.
Lesta, P., Ferello, R., and Chebli, G., 1980, Chubut extraandino, *in* Proceedings, Segundo Simposio de Geología Regional Argentina, Academia Nacional de Ciencias, Córdoba, 8–11 September, v. 2: Córdoba, Argentina: Asociación Geológica Argentina, p. 1307–1380.

López de Luchi, M.G., and Cerredo, M.E., 2008, Geochemistry of the Mamil Choique granitoids at Rio Chico, Río Negro, Argentina: Late Paleozoic crustal melting in the North Patagonian Massif: Journal of South American Earth Sciences, v. 25, p. 526–546, doi:10.1016/j.jsames.2007.05.004.

Macdonald, D., Gomez-Perez, I., Franzese, J., Spalletti, L., Lawver, L., Gahagan, L., Dalziel, I., Thomas, C., Trewin, N., Hole, M., and Paton, D., 2003, Mesozoic break-up of SW Gondwana: Implications for regional hydrocarbon potential of the southern South Atlantic: Marine and Petroleum Geology, v. 20, p. 287–308, doi:10.1016/S0264-8172(03)00045-X.

Mainprice, D., Bouchez, J.-L., Blumenfeld, P., and Tubia, J.M., 1986, Dominant *c* slip in naturally deformed quartz: Implications for dramatic plastic softening at high temperature: Geology, v. 14, p. 819–822, doi:10.1130/0091-7613(1986)14<819:DCSIND>2.0.CO;2.

Márquez, M.J., Massaferro, G.I., Fernández, M.I., Menegatti, N., and Navarrete, C.R., 2011, El centro volcánico Sierra Grande: Caracterización petrográfica y geoquímica del magmatismo extensional liásico, noreste de la Patagonia: Revista de la Asociación Geológica Argentina, v. 68, p. 555–570.

Marshall, J.E.A., 1994, The Falkland Islands: A key element in Gondwana paleogeography: Tectonics, v. 13, p. 499–514, doi:10.1029/93TC03468.

Martin, A.K., 2007, Gondwana breakup via double-saloon-door rifting and seafloor spreading in a backarc basin during subduction rollback: Tectonophysics, v. 445, p. 245–272, doi:10.1016/j.tecto.2007.08.011.

McNulty, B.A., Tobisch, O.T., Cruden, A.R., and Gilder, S., 2000, Multistage emplacement of the Mount Givens pluton, central Sierra Nevada batholith, California: Geological Society of America Bulletin, v. 112, p. 119–135, doi:10.1130/0016-7606(2000)112<119:MEOTMG>2.0.CO;2.

Miller, H., 1983, The position of Antarctica within Gondwana in the light of Palaeozoic orogenic development, *in* Oliver, R.L., James, P.R., and Jago, J.B., eds., Antarctic Earth Science: Cambridge, UK, Cambridge University, p. 579–581.

Moyen, J.F., Nédélec, A., Martin, H., and Jayananda, M., 2003, Syntectonic granite emplacement at different structural levels: The Closepet granite, South India: Journal of Structural Geology, v. 25, p. 611–631, doi:10.1016/S0191-8141(02)00046-9.

Mussett, A.E., and Taylor, G.K., 1994, ^{40}Ar-^{39}Ar ages for dykes from the Falkland Islands with implications for the break-up of southern Gondwanaland: Journal of the Geological Society, v. 151, p. 79–81, doi:10.1144/gsjgs.151.1.0079.

Neves, S.P., Araújo, A.M.B., Correia, P.B., and Mariano, G., 2003, Magnetic fabrics in the Cabanas Granite (NE Brazil): Interplay between emplacement and regional fabrics in a dextral transpressive regime: Journal of Structural Geology, v. 25, p. 441–453, doi:10.1016/S0191-8141(02)00003-2.

Olivier, P., Druguet, E., Castaño, L.M., and Gleizes, G., 2016, Granitoid emplacement by multiple sheeting during Variscan dextral transpression: The Saint-Laurent–La Jonquera pluton (Eastern Pyrenees): Journal of Structural Geology, v. 82, p. 80–92, doi:10.1016/j.jsg.2015.10.006.

Pankhurst, R.J., 1990, The Paleozoic and Andean magmatic arcs of West Antarctica and southern South America, *in* Kay, S.M., and Rapela, C.W., eds., Plutonism from Antarctica to Alaska: Geological Society of America Special Paper 241, p. 1–8, doi:10.1130/SPE241-p1.

Pankhurst, R.J., Rapela, C.W., Fanning, C.M., and Márquez, M., 2006, Gondwanide continental collision and the origin of Patagonia: Earth-Science Reviews, v. 76, p. 235–257, doi:10.1016/j.earscirev.2006.02.001.

Paterson, S.R., Vernon, R.H., and Tobisch, O.T., 1989, A review of criteria for the identification of magmatic and tectonic foliations in granitoids: Journal of Structural Geology, v. 11, p. 349–363, doi:10.1016/0191-8141(89)90074-6.

Proserpio, C.A., 1978, Descripción geológica de la Hoja 42d, Gastre, Provincia del Chubut: Secretaría del Estado de Minería, Ministerio de Economía Boletín 159, scale 1:200,000, 75 p.

Prouteau, G., and Scaillet, B., 2003, Experimental constraints on the origin of the 1991 Pinatubo dacite: Journal of Petrology, v. 44, p. 2203–2241, doi:10.1093/petrology/egg075.

Rapela, C.W., and Pankhurst, R.J., 1992, The granites of northern Patagonia and the Gastre Fault System in relation to the break-up of Gondwana, *in* Storey, B.C., Alabaster, T., and Pankhurst, R.J., eds., Magmatism and the Causes of Continental Break-Up: Geological Society of London Special Publication 68, p. 209–220, doi:10.1144/GSL.SP.1992.068.01.13.

Rapela, C.W., Dias, G.F., Franzese, J.R., Alonso, G.A., and Benvenuto, A.R., 1991, El Batolito de la Patagonia Central: Evidencias de un magmatismo triásico-jurásico asociado a fallas transcurrentes: Revista Geológica de Chile, v. 18, p. 121–138, doi:10.5027/andgeov18n2-a03.

Rapela, C.W., Pankhurst, R.J., and Harrison, S.M., 1992, Triassic "Gondwana" granites of the Gastre district, North Patagonian Massif: Transactions of the Royal Society of Edinburgh: Earth Sciences, v. 83, p. 291–304, doi:10.1017/S0263593300007975.

Rapela, C.W., Pankhurst, R.J., Fanning, C.M., and Hervé, F., 2005, Pacific subduction coeval with the Karoo mantle plume: The Early Jurassic Subcordilleran belt of northwestern Patagonia, *in* Vaughan, A.P.M., Leat, P.T., and Pankhurst, R.J., eds., Terrane Processes at the Margins of Gondwana: Geological Society of London Special Publication 246, p. 217–239, doi:10.1144/GSL.SP.2005.246.01.07.

Ribeiro, J.M., Maury, R.C., and Grégoire, M., 2016, Are adakites slab melts or high-pressure fractionated mantle melts?: Journal of Petrology, v. 57, p. 839–862, doi:10.1093/petrology/egw023.

Riley, T.R., Flowerdew, M.J., Pankhurst, R.J., Curtis, M.L., Millar, I.L., Fanning, C.M., and Whitehouse, M.J., 2016, Early Jurassic magmatism on the Antarctic Peninsula and potential correlation with the Subcordilleran plutonic belt of Patagonia: Journal of the Geological Society, v. 174, p. 365–376, doi:10.1144/jgs2016-053.

Samaniego, P., Robin, C., Chazot, G., Bourdon, E., and Cotten, J., 2010, Evolving metasomatic agent in the Northern Andean subduction zone, deduced from magma composition of the long-lived Pichincha volcanic complex (Ecuador): Contributions to Mineralogy and Petrology, v. 160, p. 239–260, doi:10.1007/s00410-009-0475-5.

Scaillet, B., and Evans, B.W., 1999, The 15 June 1991 eruption of Mount Pinatubo. I. Phase equilibria and pre-eruption *P*-*T*-fO_2-fH_2O conditions of the dacite magma: Journal of Petrology, v. 40, p. 381–411, doi:10.1093/petroj/40.3.381.

Stevenson, C., 2009, The relationship between forceful and passive emplacement: The interplay between tectonic strain and magma supply in the Rosses Granitic Complex, NW Ireland: Journal of Structural Geology, v. 31, p. 270–287, doi:10.1016/j.jsg.2008.11.009.

Stone, P., Richards, P.C., Kimbell, G.S., Esser, R.P., and Reeves, D., 2008, Cretaceous dykes discovered in the Falkland Islands: Implications for regional tectonics in the South Atlantic: Journal of the Geological Society, v. 165, p. 1–4, doi:10.1144/0016-76492007-072.

Stone, P., Kimbell, G.S., and Richards, P.C., 2009, Rotation of the Falklands microplate reassessed after recognition of discrete Jurassic and Cretaceous dyke swarms: Petroleum Geoscience, v. 15, p. 279–287, doi:10.1144/1354-079309-847.

Storey, B.C., Curtis, M.L., Ferris, J.K., Hunter, M.A., and Livermore, R.A., 1999, Reconstruction and break-out model for the Falkland Islands within Gondwana: Journal of African Earth Sciences, v. 29, p. 153–163, doi:10.1016/S0899-5362(99)00086-X.

Taylor, G.K., and Shaw, J., 1989, The Falkland Islands: New palaeomagnetic data and their origin as a displaced terrane from Southern Africa, *in* Willhouse, J.W., ed., Deep Structure and Past Kinematics of Accreted Terranes: American Geophysical Union Monograph 50, p. 59–72, doi:10.1029/GM050p0059.

Thomson, S.N., and Hervé, F., 2002, New time constraints for the age of metamorphism at the ancestral Pacific Gondwana margin of southern Chile (42–52°S): Revista Geológica de Chile, v. 29, p, 151–165.

Tikoff, B., and Greene, D., 1997, Stretching lineations in transpressional shear zones: An example from the Sierra Nevada Batholith, California: Journal of Structural Geology, v. 19, p. 29–39, doi:10.1016/S0191-8141(96)00056-9.

Tobisch, O.T., McNulty, B.A., and Vernon, R.H., 1997, Microgranitoid enclave swarms in granitic plutons, central Sierra Nevada, California: Lithos, v. 40, p. 321–339, doi:10.1016/S0024-4937(97)00004-2.

Tullis, J., Stünitz, H., Teyssier, C., and Heilbronner, R., 2000, Deformation microstructures in quartzo-feldspathic rocks, *in* Jessell, M.W., Urai, J.L., eds., Stress, Strain and Structure: A Volume in Honour of W.D. Means: Journal of the Virtual Explorer, v. 2, 16, doi:10.3809/jvirtex.2000.00019.

Uliana, M.A., and Biddle, K.T., 1987, Permian to late Cenozoic evolution of northern Patagonia: Main tectonic events, magmatic activity, and depositional trends, *in* McKenzie, G.D., ed., Gondwana Six: Structure, Tectonics, and Geophysics: American Geophysical Union Monograph 40, p. 271–286, doi:10.1029/GM040p0271.

Uliana, M.A., and Legarreta, L., 1999, Jurásico y Cretácico de la cuenca del Golfo de San Jorge, *in* Caminos, R., ed., Geología Argentina: Subsecretaría de Minería de la Nación, Servicio Geológico Minero Argentino, Instituto de Geología y Recursos Minerales, p. 496–510.

Vaughan, A.P.M., and Livermore, R.A., 2005, Episodicity of Mesozoic terrane accretion along the Pacific margin of Gondwana: Implications for superplume-plate interactions, *in* Vaughan, A.P.M., Leat, P.T., and Pankhurst, R.J., eds., Terrane Processes at the Margins of Gondwana: Geological Society of London Special Publication 246, p. 143–178, doi:10.1144/GSL.SP.2005.246.01.05.

Vicente, J.C., 2005, Dynamic paleogeography of the Jurassic Andean Basin: Pattern of transgression and localisation of main straits through the magmatic arc: Revista de la Asociación Geológica Argentina, v. 60, p. 221–250.

Vigneresse, J.L., 1995, Control of granite emplacement by regional deformation: Tectonophysics, v. 249, p. 173–186, doi:10.1016/0040-1951(95)00004-7.

Vigneresse, J.L., and Bouchez, J.L., 1997, Successive granitic magma batches during pluton emplacement: The case of Cabeza de Araya (Spain): Journal of Petrology, v. 38, p. 1767–1776, doi:10.1093/petroj/38.12.1767.

von Gosen, W., 2002, Polyphase structural evolution in the northeastern segment of the North Patagonian Massif (southern Argentina): Journal of South American Earth Sciences, v. 15, p. 591–623, doi:10.1016/S0895-9811(02)00111-6.

von Gosen, W., 2003, Thrust tectonics in the North Patagonian Massif (Argentina): Implications for a Patagonia plate: Tectonics, v. 22, 1005, doi:10.1029/2001TC901039.

von Gosen, W., 2009, Stages of Late Palaeozoic deformation and intrusive activity in the western part of the North Patagonian Massif (southern Argentina) and their geotectonic implications: Geological Magazine, v. 146, p. 48–71, doi:10.1017/S0016756808005311.

von Gosen, W., and Loske, W., 2004, Tectonic history of the Calcatapul Formation, Chubut province, Argentina, and the "Gastre fault system": Journal of South American Earth Sciences, v. 18, p. 73–88, doi:10.1016/j.jsames.2004.08.007.

Yoshinobu, A.S., Wolak, J.M., Paterson, S.R., Pignotta, G.S., and Anderson, H.S., 2009, Determining relative magma and host rock xenolith rheology during magmatic fabric formation in plutons: Examples from the middle and upper crust: Geosphere, v. 5, p. 270–285, doi: 10.1130/GES00191.1.

Zaffarana, C.B., and Somoza, R., 2012, Paleomagnetism and $^{40}Ar/^{39}Ar$ dating from Lower Jurassic rocks in Gastre, central Patagonia: Further data to explore tectonomagmatic events associated with the breakup of Gondwana: Journal of the Geological Society, v. 169, p. 371–379, doi:10.1144/0016-76492011-089.

Zaffarana, C.B., López de Luchi, M.G., Somoza, R., Mercader, R., Giacosa, R., and Martino, R.D., 2010, Anisotropy of magnetic susceptibility study in two classical localities of the Gastre Fault System, central Patagonia: Journal of South American Earth Sciences, v. 30, p. 151–166, doi:10.1016/j.jsames.2010.10.003.

Zaffarana, C.B., Montenegro, T., and Somoza, R., 2012, The host rock of the Central Patagonian Batholith in Gastre: Further insights on the Late Triassic to Early Jurassic deformation in the region: Revista de la Asociación Geológica Argentina, v. 69, p. 106–126.

Zaffarana, C.B., Somoza, R., and López de Luchi, M., 2014, The Late Triassic Central Patagonian Batholith: Magma hybridization, $^{40}Ar/^{39}Ar$ ages and thermobarometry: Journal of South American Earth Sciences, v. 55, p. 94–122, doi:10.1016/j.jsames.2014.06.006.

Žák, J., Schulmann, K., and Hrouda, F., 2005, Multiple magmatic fabrics in the Sázava pluton (Bohemian Massif, Czech Republic): A result of superposition of wrench-dominated regional transpression on final emplacement: Journal of Structural Geology, v. 27, p. 805–822, doi:10.1016/j.jsg.2005.01.012.